



Using Machine Learning with Scanning Sonar Data and Artificial Targets for Shrimp Biomass Estimation

Hamzah Isap

School of Engineering, Lancaster University

August 2025

This thesis is submitted for the degree of:

MSc by Research Engineering

Abstract

Smart aquaculture is a data-driven approach to optimise operations and is a valuable practice for shrimp farmers to upscale sustainably. Acoustic telemetry is generally regarded as the most reliable form of data acquisition to obtain desired stock information, such as biomass and abundance. Current studies in the field deploy high-grade scientific sonars and their data to train sophisticated models, overlooking the financial viability. In contrast, this study explores the potential for basic-specification single-beam scanning sonars to construct acoustic datasets for model training. We propose separate methods for using machine learning to predict two stock measurements: school density and abundance, using artificial targets in a sample area. To model school density, a monofilament net containing a varied density of standardised uniform air-filled spheres produces echo traces, which an optimised neural network categorises to an overall accuracy of 90.78%. To model shrimp abundance, artificial targets modelling shrimp are presented to capture abundance with active material and orientation variables. We collect averaged echograms of the tank containing a variable abundance of suspended targets. We then deploy a variation of echo-integration where the sum of digital signals for each beam position is processed as features. Optimised Gaussian process regression models are the best-performing models in predicting the number of targets in the tank. Training models on different population ranges found the maximum error around 10%, with the best model demonstrating an MAE of 1.36 (2.7%). Models fit data with an R-squared upwards of 0.98. The proposed methods demonstrate the promising potential of low-cost sonar implementation within the aquaculture industry.

Table of Contents

Abstract	i
List of Abbreviations	iii
List of Tables	iv
List of Figures	iv
Acknowledgements	V
Author's Declaration	vi
1. Introduction	1
2. Literature Review	5
2.1. Aquaculture and Shrimp Farming	5
2.1.1. Sustainability Challenges	5
2.1.2. The Shrimp Farming Process	6
2.1.3. Biomass Estimation, Precision Farming and Smart Aquaculture	8
2.2. Sonar Technology and Key Underwater Acoustic Concepts	10
2.2.1. Acoustic Technology as a Biomass Estimation Method	11
2.2.2. Operating Principles of Sonar Technology and Its Evolution	12
2.2.3. Acoustic Waves and Target Strength	13
2.2.4. Beamforming and Horizontal Propagation	15
2.2.5. Echo Counting and Integration	17
2.3. Evaluating Sonar Systems and Machine Learning Techniques	18
2.3.1. Comparing Acoustic Systems	18
2.3.2. Machine Learning Techniques	19
2.3.3. Acoustic Data Acquisition	21
2.3.4. Analysing Acoustic Shrimp Data	22
2.3.5. Financial Viability of Sonar Systems	24
3. Methods and Materials	26
3.1. Operating Principles of the BRS-1	26
3.2. Visualising Acoustic Data	26
3.3. Method Process Flow	27
3.4. Estimating School Density	28
3.4.1. Study Design	28
3.4.2. Dataset Construction and Pre-Processing	29
3.4.3. Data Analysis	30
3.5. Fetimating Abundance	21

3.5.1. Study Design	31
3.5.2. Dataset Construction	33
3.5.3. Data Analysis	34
4. Results	35
4.1. Estimating School Density	35
4.1.1. Evaluating Classifier Performance	35
4.1.2. Evaluating Performance using Data from Optimised Sonar	36
4.2. Estimating Abundance	38
5. Discussion	41
6. Conclusion and Recommendations	44
Appendices	45
Appendix 1 – Hardware Features of OTAQ's BRS-1	45
Appendix 2 – Sonar Visualisation Code	50
Appendix 3 – Echogram Timelapse Code	55
References	57

List of Abbreviations

Abbreviation	Meaning
Al	Artificial Intelligence
ANN	Artificial Neural Network
DAQ	Data Acquisition
DL	Deep Learning
DWBA	Distorted Wave Born Approximation
FNR	False Negative Rate
GAN	Generative Adversarial Network
GPR	Gaussian Process Regression
IoT	Internet of Things
KNN	K-Nearest Neighbours
MAE	Mean Absolute Error
MBES	Multibeam Echosounder
ML	Machine Learning
MLP	Multilayer Perceptron
PCA	Principal Component Analysis
RF	Random Forest
RMSE	Root Mean Square Error
TPR	True Positive Rate

Abbreviation	Meaning
TS	Target Strength
TVG	Time-Varied Gain
YOLO	You Only Look Once
List of Tables	
Table 2 – Accuracies of Table 3 – Improved accuracies of Table 4 – Performance target dataset	of models predicting sphere number
List of Figures	
Figure 2 – Smart aqual Figure 3 – Single bear Figure 4 – General profigure 5 – Echogram of Figure 6 – Schematic Figure 7 – (i) Experime Figure 8 – Bounding bound figure 9 – Artificial tar Figure 10 – Backscatt Figure 11 – Net overlawire	farming process [28], [30]
_	matrix with true positive and false negative rates of the second
Figure 14 – Residual p Figure 15 – Schematic Figure 16 - Sonar data Figure 17 - Sonar data	olot when tested on a 50-target density

Acknowledgements

This research was made possible by the financial and logistical support of the Innovate UK-funded Centre for Digital Innovation programme in collaboration with Lancaster University.

I wish to thank Dr Alex Bush for his continuous guidance and supervision throughout the project. I want to express my sincere gratitude to Dr Peter Robinson for his support as both an academic and industry collaborator. Thank you for graciously providing the space and resources needed to conduct the research and for answering my questions on acoustics and electronics.

Thanks to OTAQ for providing the sonar, and to the rest of the team, particularly Tony Jakas and Joe Dowswell, for their technical and software support. Additional thanks go to Wayne Stevens and Tom Newby for their assistance in the lab.

Thanks to Dr Belinda Yaxley for answering my queries on shrimp behaviour and aquaculture. Many thanks to the University and staff involved in the programme, including Dr Rebecca Robinson.

Finally, a special thanks to my family. To Mum and Dad, I cannot thank you enough for your unwavering support and encouragement throughout this journey. Thank you for always believing in me, even when I doubted myself.

Author's Declaration

I declare that this project is my own work and has not been submitted in substantially

the same form towards the award of a degree or other qualificatory work and affirm that

acknowledgement has been made to assistance given and that all major sources have

been appropriately referenced.

Signed: X

Hamzah Isap

Date: 01/08/2025

vi

1. Introduction

The globalisation of the aquaculture industry is a response to dramatic shifts in nutritional demand [1]. The multifaceted opportunities for developing countries have driven the rapid expansion of shrimp farming operations [2]. However, due to poor and unregulated planning, socioeconomic and environmental ramifications have arisen, including the destruction of mangrove areas, coastal lowlands, and other rich, biodiverse ecosystems [3], [4]. Increased profitability has been achieved through land footprint expansion rather than optimising operations [5]. Upscaling sustainable aquaculture activities has been challenging due to inefficient feeding, resulting in nitrous waste, high operating costs, and low yields attributed to high mortality rates [6]. The need for formulated feed in the grow-out phase is a major source of production costs [7], with the production cycle in shrimp ponds averaging around 25 weeks wherein 1-2 g animal grow out to a harvest weight of 20-27 g [8]. Thus, feed scheduling is a critical area for improvement, as its optimisation would significantly enhance the overall process. The lack of insight into the growth, behaviour and abundance of stock under murky and turbid waters means farmers cannot adapt maintenance strategies to changes in biomass. Traditional monitoring and stock assessment methods have attempted to overcome this; however, manual techniques, such as trawling and occasional video monitoring [9], are labour-intensive, time-consuming, inaccurate and invasive [10]. Precision farming techniques were introduced to collect data on stock in ponds using Data Acquisition (DAQ) systems and statistical analysis [11], [12]. De Rosny and Roux first proposed fish monitoring methods using acoustic measurements, analysing back-scattering cross-sections using a reverberation time-series [13], with further studies employing the same fundamentals. Whilst these methods can yield impressive biomass estimations, they are challenging to apply commercially due to their statistically intensive nature and difficulty in replicating. In recent years, research has proposed developing fast, accurate and automated biomass estimation methods to optimise farming processes.

Smart aquaculture is a new scientific field that aims to develop digital solutions that convert large volumes of complex data into easily understandable and actionable information. The approach supports data-driven, knowledge-based decision-making, optimising the maintenance of commercial ponds to improve resource management and harvest [14]. Several DAQ systems have been proposed to facilitate the philosophy in aquaculture ponds, including machine vision and sensor-based technology [6], [15]; however, the challenging environment of shrimp ponds makes it difficult to obtain high-quality data. Sonar technology is showing the most promise for DAQ in shrimp pond environments [16], [17]. Its superiority over other proposed methods comes from its high range underwater and suitability against light attenuation in turbid water. Sonar technology is also versatile, as devices can be designed to overcome financial constraints, making it an appealing, cost-effective option if performance can be achieved. Shrimp farms often utilise extensive (i.e., 1–10 shrimp/m²), semi-intensive (10–25 shrimp/m²), and intensive (>25 shrimp/m²) production strategies [9]. While these densities can create overlapping echoes that are difficult to analyse individually, techniques such as echo-integrator regression can be employed to estimate abundances by analysing the entire sample volume [18],[19]. The advancement of Artificial Intelligence (AI), particularly Machine Learning (ML), has revolutionised industrial processes across sectors by deriving new knowledge from existing data. Techniques such as Random Forest (RF) Algorithms, K-Nearest Neighbours (KNN), and Artificial Neural Networks (ANNs) have shown success, being easy to implement commercially by supplementing DAQ systems [20]. This underpins the prospect of developing ML models to extract measurements from aquaculture data, thereby achieving efficient farming.

Previous sonar and ML studies have been successful in fishery acoustics. Lin et al. [21] successfully developed a YOLOv4 (You Only Look Once) network that identified the number of white shrimps from 1 to 4 and their orientations, whilst Pargi et al. were able to predict fish biomass in murky water using Deep Learning (DL) of sonar images using an ARIS Explorer 3000 device and ARIScope software [22]. Minelli et al. [23] used KNN to detect and classify fish schools; Proud et al.

[24] used RF classifiers for silver cyprinid. One of the biggest challenges when scaling up ML-based approaches is the time-consuming nature of acquiring the needed data to construct a well-balanced dataset [16]. The difficulty in obtaining data from dynamic organisms hinders the development of robust analysis methods, thereby stagnating research progress. Therefore, alternate and novel methods of acquiring data are needed to validate ML techniques on acoustic data before they are deployed in commercial farms. Additionally, despite its suitability, sonar remains a high noise, low resolution system especially when horizontally propagating in shallow water due to the reverberation from surface and ground reflections. Further factors like the Doppler effect, multiple echo paths, sidelobe interference and internal device noise can degrade data quality by obscuring real signals, making it challenging to distinguish targets from the background [16]. As such, reliable methods are needed to preprocess acoustic data to manage these limitations, cleaning the data to enable feature extraction. Finally, studies to date have relied on high-tech instruments to facilitate their work, which can be expensive. These sonars are priced out of reach [25] for farmers interested in incorporating new technologies for biomass estimation, and as such, they are not viable for most aquacultural applications. Low-cost sonar technology is readily available on the market; examples of these include mechanically driven scanning sonars [26]. Clearly, research is needed to investigate whether low-cost sonars can produce satisfactory data for ML techniques to extract valuable insights for shrimp farmers, as this is the only viable avenue that may lead to commercial implementation.

This study explores the potential for low-cost sonar to contribute to routine stock assessment in commercial shrimp farms. The study aims to estimate sonar performance in field environments by varying the abundance, position, and material of targets in a controlled environment and evaluating the accuracy of machine learning models. We propose data acquisition techniques that simulate shrimp distribution data using artificial targets and placement methods. The study explores alternative data preprocessing techniques, and we apply data analysis techniques in the context of the spatial intensity data produced by the scanning

sonar. The above applies to finding two separate insights in the context of shrimp farming: school density and abundance, using ML models. These investigations should help determine whether low-cost scanning sonars are suitable for smart shrimp farming and whether on-field testing is an appropriate next step.

2. Literature Review

2.1. Aquaculture and Shrimp Farming

The growing global demand for food, driven by a rapidly expanding population, has led to a shift in dietary patterns as regions search for alternative sources of nutrition to address the emerging deficit. This has been experienced at an accelerated rate in several pockets of the world, with environments suitable for aquacultural expansion increasing the share of their nutrition through seafood [1]. Aquaculture has made significant contributions to global food security, with shrimps emerging as one of the most valuable seafood products in worldwide trade [27], with global production increasing by 86% in the past 10 years, reaching more than 6.5 million tonnes of shrimp in 2019, valued at nearly 40 billion US dollars [5]. The most commercially valuable species produced in aquaculture is Litopenaeus vannamei, which constitutes 70% of industry production [9]. The multibillion-dollar business has attracted developing countries as a way to generate profits, local employment and currency to significant effect [2]. In such countries, shrimp aquaculture has yielded significant socioeconomic benefits, with the generation of foreign exchange serving as the driving force behind rapid expansion. Although it is possible to operate with high stocking densities of shrimp, commercial strategies often utilise lower densities, including extensive (i.e., 1–10 shrimp/m²), semi-intensive (10–25 shrimp/m²), and intensive (>25 shrimp/m²) production [9]. The exponential growth has led to negative consequences due to poor planning and a lack of regulations, resulting in environmental impacts, waste and social conflicts [3] that require urgent solutions through effective management techniques.

2.1.1. Sustainability Challenges

Shrimp farming can have environmental impacts based on (1) the location of shrimp pond construction and (2) the management and technology used during shrimp pond operations, among others [4]. The particularly rapid development in countries such as Bangladesh, Vietnam, China, Thailand and Ecuador has led to expansions in activity at the expense of tropical and subtropical lowlands, endangering ecosystems. As of 2001, approximately 1–1.5 million hectares of

coastal lowlands had been converted into shrimp ponds, consisting mainly of mangrove areas, marshes, agricultural lands and salt flats [4], degrading biodiversity. In addition, poor and excess feed quality has been cited as a main source of pollution [3], [27], with the organic matter reacting with the environment's pH, temperature and pressure. The creation of ponds also impacts natural processes such as water runoff and sedimentation, creating a ripple effect that hinders the growth of trophic structures and introduces contaminants and trace elements. To combat this, an influx of research has been conducted since the turn of the century, proposing management techniques to reduce footprint expansion by streamlining the farming processes. Emerencio et al. proposed intensification of cultures, creating high-density production and greater use of existing infrastructure [5]. This involves implementing higher levels of feeding, aeration, and labour, which further emphasises the influence of these variables on production. Hossain et al. proposed several recommendations to manage the impact in Bangladesh, including coastal zoning and establishing Environmental Impact Assessments [3]. Whilst these steps are undoubtedly effective in mitigating the impacts of expansion, additional solutions are required to streamline current processes with minimal changes to operating methods that can bring immediate improvements to resource management.

2.1.2. The Shrimp Farming Process

Generally, the shrimp farming process follows 4 distinct stages from hatchery to harvest, as shown in Figure 1. The procedure can vary depending on the philosophies employed, such as those used in indoor versus outdoor environments. Cultivating broodstock spawn to post larvae for stocking in growout ponds requires strict monitoring within specialised tanks, typically indoors [28], [29]. The hatchery and nursing phases are arguably the most crucial stages in the process, and extensive methods and research have been well-established for them. Thorough management of variables such as salinity, pH, temperature, aeration, and feeding has left little to be improved upon in the pre-grow-out phases. If more efficient practices and sustainable output are to be observed, solutions need to optimise procedures in the grow-out phases.



Figure 1 – The shrimp farming process [28], [30]

Whilst plentiful research has been conducted to improve growth conditions [2], [5], [28], [29], a significant inefficiency in the process remains in the method of feeding and adapting to unexpected changes in stock. Scaling up aquaculture activity has presented challenges as farmers cope with issues that threaten to make the process considerably less efficient in terms of time, cost, and yield. Shrimp farmers experience these challenges on a wide scale when they attempt to feed growing shrimp the optimal amount of foodstuff and harvest shrimp at the best biomass [6]. The need for formulated feed in the grow-out phase is a major source of production costs in shrimp farming. Thus, the quantity of feed used relative to the yield harvested is a key metric in evaluating economic success within a commercial cycle [7]. Maintaining stock with feed at this stage is the most time- and labour-intensive stage of production, with manual monitoring being a significant drain on resources. Shrimp behaviour is often observed through visual inspection or by using video recordings, which are infrequent so as not to disturb the livestock [9]. However, these methods are often still ineffective in capturing the condition of shrimp or in detecting early signs of disease. Optimising feed and the grow-out process will improve yield within commercial ponds, allowing farmers to meet demand without undertaking damaging pond expansions. The introduction of easy-to-implement telemetry is needed to reduce the workload of farm operators while enhancing insights with minimal effort.

2.1.3. Biomass Estimation, Precision Farming and Smart Aquaculture

Farmers can derive key stock assessment information through biomass estimation. The practice is the most common and significant way of controlling stocking density, optimising feeding and determining the optimal time for harvesting [6]. The ability to achieve this is commonly referred to as precision farming. Until now, estimating marine biomass has relied on manual sampling techniques, such as trawling and subsampling, to determine the average weight of the stock. Feed trays can also be inspected to calculate feeding rates [31], [32]. These processes can be time-consuming, invasive and potentially misleading, with an inherent inaccuracy of 15-25% [10]. To solve this, research has been aimed at developing fast, accurate, and non-invasive techniques for estimation without the need for manual intervention. Studies to develop technological solutions have seen unprecedented interest in aquaculture, with researchers employing various tools to provide a proof of concept of the data that can be collected to help estimate biomass. Initially, solutions utilising technology opted for statistical analysis using surveying techniques and acoustic methods [11], [12]. De Rosny and Roux first described acoustic methods for monitoring fish behaviour using time-series coherent intensity backscatter and decay equations with ultrasonic transducers [13]. The results showed positive applications, underscoring the potential for valuable insights being gained about marine life in environments previously deemed challenging to monitor. These early studies were crucial in laying the foundation for precision farming and the current emerging trend. A limitation that prevented these early iterations from being commercially implemented was their statistically intensive nature, which is also time-consuming and complex to repeat in less sophisticated operations. Additionally, data would require validation based on catch results, making the process dependent on manual input. This led researchers to develop automated analysis methods, building on precision farming techniques in a new scientific field commonly referred to in literature as smart aquaculture. While the terms smart aquaculture and precision farming are often interchanged, their continued mention here will adhere to the outlined definitions.

Smart aquaculture aims to create digital solutions that can process large volumes of complex data into easily understandable and actionable information. This approach enables data-driven, knowledge-based decision-making, streamlining the maintenance of commercial ponds to achieve improved yields [14]. Data insights, such as abundance, length, biomass, and behavioural information, can also enable efficient resource usage in the grow-out phases, creating sustainable aquacultural activities and improved financial performance, which is summarised in Figure 2 [33]. The breakthrough of AI, particularly ML techniques, has revolutionised a vast majority of industries, not limited to healthcare, manufacturing, energy and sales [20]. Consequently, the application of ML serves as the critical tool for transforming processes and is designed to derive knowledge from existing data [34]. It stands to reason that ML is the key to unlocking smart aquaculture, with its subset, Deep Learning (DL), being the focus at the cutting edge of the field. Proposed DL methods have most recently been enhanced with infrastructure capable of handling automated tasks in real time using cloud computing, big data, and the Internet of Things (IoT) [33] Whilst that is vital research, the lack of definitive ML applications in this particular field means that further foundational research is required to evaluate the challenges posed in applying ML to shrimp farming.

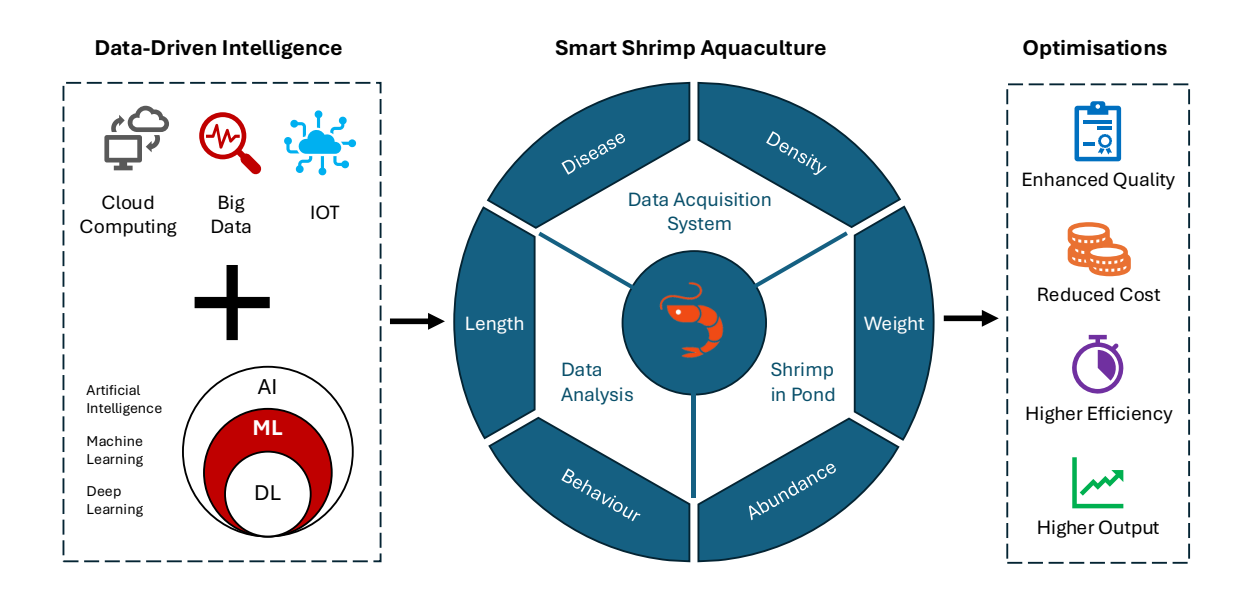


Figure 2 - Smart aquaculture principles applied to shrimp farming [33]

Several comprehensive reviews have been conducted to evaluate the effectiveness and suitability of technologies for smart aquaculture. The main techniques pursued here include [6], [15]:

- Machine vision: Using a monocular or stereovision optical light camera setup at the surface, analysing image data.
- 2. **Acoustics**: Acquiring data from sound propagation using sonar, echosounders or passive equipment.
- Sensor-based technologies: Measuring pass-throughs using resistivity counters with electrodes or infrared beams.

Investigations into these tools are relatively new. Literature reviews suggest there is limited research and development on smart aquaculture [6]. Hence, it remains unclear what the definitive best technology is for this application, considering the close exchange of benefits and drawbacks associated with adopting each. This is likely due to the absence of studies proposing methods to extract insights from the data of these devices. More systematic methods utilising these technologies effectively need to be published to promote techniques superior to manual sampling.

2.2. Sonar Technology and Key Underwater Acoustic Concepts

Comprehensive research focused on individual technologies can help determine the best data acquisition systems and ML techniques for shrimp farming. Industry collaborators, OTAQ, have developed a mechanically driven sonar device, providing an opportunity to investigate the capabilities and limitations of hydroacoustic methods. The device relies upon acoustic principles, which are critical when analysing data output and explaining experimental results. Acoustic sensor principles can be compared well with optical devices. This is due to the similarity between the theories of sound and light [18], with many phenomena being observed in both, such as absorption, reflection, and scattering. Acoustic waves propagate over long distances in water, a superior medium for sound propagation due to the liquid's increased conductivity.

2.2.1. Acoustic Technology as a Biomass Estimation Method

Within the field of underwater object detection, there has been a recent rise in the popularity of acoustic techniques and devices that form the backbone of potential solutions. This comes after a previous trend in scholars focusing on alternate methods such as computer vision, machine vision, resistive sensor technology and tagging [15]. While these methods are still being pursued in other contexts, it is evident from multiple research teams [16]-[18], [35] that there is reason to suggest that acoustic techniques offer an overall superior use case in shrimp aquaculture for several reasons. These include:

- The non-intrusive nature of sonar and acoustic technology
- The high range of sound waves propagating in water
- Reliability in highly turbid waters
- Suitability in areas of minimal light
- The scope for cost-effective solutions

In any study involving marine life and aquaculture monitoring, one of the critical considerations is the feasibility of operating while minimising the negative impact on the measured live specimens. For aquacultural farmers, it is imperative that the stock is not put under increased stress, as this can directly cause several other abnormalities, such as shorter lifespans, increased mortality levels, and poor growth rates [6]. Whilst other monitoring systems, such as resistive sensory technology, may provide key insights that acoustic technology cannot, its intrusive nature can diminish any benefit its deployment offers. Acoustic technology's range means that devices can be installed away from activity, enabling data acquisition without affecting the ecosystem's natural behaviours or causing injury.

The robust nature of sound waves propagating in highly turbid waters means that acoustic systems produce reliable information [36]. This factor becomes crucial during the design stage when considering other systems reliant upon alternate mediums such as visible light and other electromagnetic waves. Machine vision solutions in research have been shown to provide information on the behaviour, swimming, and body orientation of shrimp [17]. Although it can be argued that

systems such as computer and machine vision produce image details better than sonar, their susceptibility to light attenuation and refraction in turbid waters increases with depth, meaning that the quality of these images can significantly deteriorate in detail [16], [35]. This is particularly emphasised when considering how most shrimp species position themselves in the lowest layer of a body of water, known as the benthic zone [35]. This makes using acoustic telemetry vastly more appealing when designing a solution that can be semi-permanently operated unsupervised and remotely.

2.2.2. Operating Principles of Sonar Technology and Its Evolution

A Sonar device can detect objects underwater from their physical attributes and the water medium [6]. Like all other systems that rely upon the principles of underwater sound, a sonar converts mechanical energy propagated via sound wave into an electrical signal when the wave reaches the receiver. Acoustic devices can be split into two primary groups – active and passive [16]. A passive system detects objects with a receiving array and is used to discover sound sources, requiring the object concerned to emit sound waves. These are often referred to as hydrophones. On the other hand, active acoustics produce sound waves from a transmitting array and use a receiving array to detect objects. An electrical signal is applied to a transducer, which converts the pulse into a mechanical vibration that produces an oscillating pressure and results in an acoustic wave [17]. The wave propagates in the water and scatters once it interfaces with a different medium. This results in a portion of the original wave being reflected to a receiving transducer. The pressure from the echo pulse excites the transducer [37], resulting in an electrical signal which conveys information about the backscattered wave. The return signal can be processed digitally to form data which provides insight into the object's physical characteristics through properties such as amplitude and distance.

The evolution of modern sonar can be traced back to World War II [6], [38]. As such, acoustic technology has seen substantial advancements, creating a range of iterations varying in complexity and cost. The simplest form of sonar is an active single-beam echosounder [17] that is still commonly used to measure range and

depth. Dual-beam sonars were introduced in the 1970s, adding a second dimension to measurements. The 1980s brought split-beam sonars, which added a third dimension to the data acquired. Multibeam echosounders (MBES) were introduced to provide precise, higher-resolution data, allowing the spatiotemporal attributes of the scanned area to be captured. The recent advancements in acoustic technology mean the technique rivals other methods that are notable for their precision and data quality. The production of refined video-like sonar images allows for the deployment of supervised machine learning-based classifiers that can be successfully trained and deployed for object detection, species identification, biomass estimation, automatic counting, and length measurements [15]. ML classifiers can use protocols similarly applied to regular optical images and videos. Unlike most technological advancements that render predecessors obsolete, sonar development has created a spectrum of configurations to explore, finding an ideal set that balances cost and capability.

2.2.3. Acoustic Waves and Target Strength

Acoustic waves are mechanical oscillations. When a wave passes through a substance, it experiences local changes in density and mass displacement. This results in a counteractive force induced by the medium to bring the density back to equilibrium [39]. The phenomenon complies with Newton's second law, the conservation of mass, and the relationship between pressure and volume. Thus, it can be expressed as the linear acoustic wave equation (1):

$$\nabla^2 p = \frac{1}{c^2} \frac{\delta^2 p}{\delta^2 t} \tag{1}$$

Where ∇^2 is the Laplace operator, p is the pressure over t, time. c is the speed of sound in ambient conditions.

The acoustic wave equation explains a wave's interaction with varying objects, whose principal properties are volume stiffness, K, and density, ρ , with the properties impacting sound speed as (2):

$$c = \sqrt{\frac{\kappa}{\rho}} \tag{2}$$

The intensity of an acoustic wave is the critical feature that a wave carries when it backscatters as an echo. Backscatter occurs whenever there is a spatial change [18] in the acoustic impedance, Z (3):

$$Z = \rho c \tag{3}$$

The greater the change in Z across a boundary (i.e. between the water and a target), the stronger the backscattered wave. This is a result of a greater proportion of the entire transmitted wave being reflected, with the remainder continuing as transmitted, often referred to as forward scatter. The intensity, I, describes the product of a wave's instantaneous pressure and particle velocity. This can convey information about a target's density and volume stiffness from a wave reflected from it.

$$I = \frac{p^2}{\rho c} \tag{4}$$

The pressure intensity of acoustic waves can convey a plethora of information and forms the basis of unit measurements expressing the objects interacting with the sonar. The extent to which an echo signal resembles the intensity of the whole signal depends on how reflective the ensonified target is. This acoustic property of an object is referred to as the backscattering cross-section (5) and can be quantified by calculating the ratio of intensities between the incident and reflected signal [38], [18].

$$\sigma_{bs} = \frac{l_r}{l_i}\Big|_{r=1} \tag{5}$$

 σ_{bs} is the backscattering cross-section

 I_r is the intensity of the reflected intensity, 1 meter from the object

 I_i is the incident intensity

The measurement can then be expressed in decibels, allowing for a larger logarithmic scale. This enables slight differences in ratio to be displayed clearly,

emphasising the effect of the changing energy reflected for different objects. As a result, the logarithmic parameter is more commonly used in hydroacoustic applications and is known as the Target Strength (TS) (6).

$$TS = 10 \log \left(\frac{l_r}{l_i}\right)\Big|_{r=1}$$
 (6)

Object reflectivity is influenced by factors such as signal characteristics, the propagation medium, and the object itself. Despite the complexities, the target strength offers valuable insights, helping acousticians identify specific targets or classify unknown ones. [40]. The valuable insight offered by the simple ratio makes target strength a popular focal point for research in the field, as scholars develop techniques and propose models that can provide a deeper understanding of target strength values. Target strength is widely considered to be a practical measurement [18] – a value derived through conducting physical measurements and empirical data. The values of target strength measured are commonly evaluated against reference sheets. Users can reliably identify the target reflected by contextual information, such as what is expected within the scanned volume. However, it is commonly accepted within research that target strength is a transient measurement sensitive to the context and environment upon which it is gathered. The frequency must be carefully considered to prevent resonance from occurring at any stage due to small changes in signal exhibiting disproportionately large changes in target strength [38]. In addition, changes in tilt angle for large objects or the orientation for small objects can also result in changes in target strength, which can be challenging to manage when scanning a dynamic environment filled with live specimens [41]. The various influences on target strength make it a problematic measurement to base precise findings on outside laboratory conditions.

2.2.4. Beamforming and Horizontal Propagation

The response of a transducer is designed to be directional, having directional sensitivity that can be expressed with a beam pattern, as shown in Figure 3 [42]. The phase differences between parts of the transducer along its dimensions result in lobes, where source points are in phase and output is maximal [18]. Alternate

null patterns are also created between the lobes as source points become out of phase, causing signals to cancel each other out. The main lobe refers to the maximum output occurring at the acoustic axis, which is located at the centre of the transducer along the axis of propagation. Experimental results [43], [44] suggest the main lobe is estimated to carry 99% of the transmitted acoustic energy of the beam. Thus, the single beam produced can be simplified as a conical beam, similar to a searchlight. The spread of the main lobe can be expressed in terms of the beam width. This refers to the distance between the two opposing sides of the main lobe at the range where it reaches its apex, and is where a 3 decibel (dB) decline in intensity is observed. The beam width describes the angular resolution of a sonar system since two targets cannot be resolved if they are closer together than the beam width. The angular resolution of a rectangular transducer with face dimensions L_x , L_y , and operating wavelength λ , can be expressed as:

$$\theta_{3Db} = \pm 25.3 \times \frac{\lambda}{L_x}, \pm 25.3 \times \frac{\lambda}{L_y} \tag{7}$$

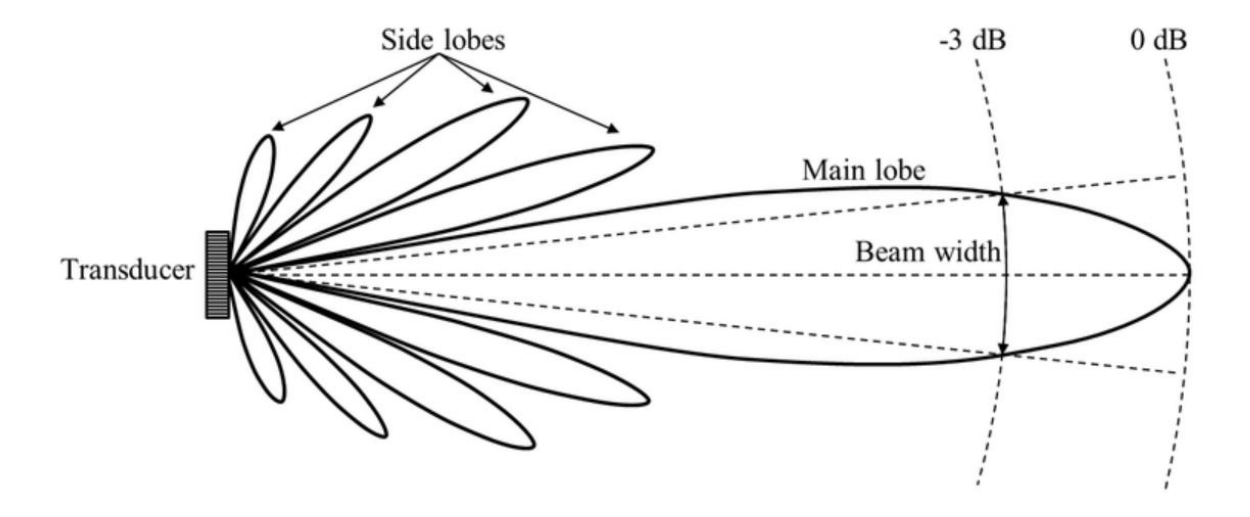


Figure 3 – Single beam transducer directional sensitivity beam pattern [42]

Horizontal acoustic propagation can be applied to shallow water, such as shrimp ponds, where areas near the surface and bottom are significant regions of interest. Horizontal beaming allows sonars to cover vast ground in a limited-depth region, with these types of surveys established in literature [45],[46], [47]. Despite this, several practical problems are experienced that are not encountered with vertical beaming. The most significant concern in this application is the boundary echoes

caused by the direct reverberation from the bottom and surface. As the beam spreads to reach these interfaces, reflections occur due to the stark acoustic impedance differential between water and air/hard floors. The reverberations from these reflections can cause noisy backgrounds, which can obscure weaker target signals more than stronger ones, resulting in data bias [18]. Furthermore, the frequent interaction of the beam with boundaries can create complex propagation paths, which can impact the pathways taken by echoes from targets. Whilst portions of echoes may take direct paths to the receiver, others from the same target may take longer reflection paths, resulting in a time delay and skewed data results. The extent to which these issues impact horizontally propagating sonars is still debated. Hence, research is needed to determine if data quality from this technique is satisfactory beyond these issues.

2.2.5. Echo Counting and Integration

It is possible to detect the echoes of individual targets when reflective targets are well separated from each other. This can be seen as a viable approach for lowdensity fish farming, where individual signals can be evaluated to collect data on individual fish. This technique is referred to as echo-counting. Signal properties can be closely analysed to develop key insights into fish morphology. Size and length measurements are valuable data estimated from a received signal in research using statistical models for target length [11],[48]. However, the environment in shrimp ponds exhibits contrasting conditions, with weakly reflecting targets at high densities, rendering echo-counting an unreliable approach. To solve this, an alternate method known as echo-integration has been proposed [49]. The technique is used to estimate abundance despite overlapping echoes. This is achieved by creating a proportionality model that relates the average integrated intensity of received signals in a defined volume to the number of targets ensonified [19]. The accumulation of echo energy can be achieved by connecting a sonar to a traditional echo-integrator unit, which sums the squares of signals and can be converted to an abundance using a scale factor and adjusting the device's Time-Varied Gain (TVG) [18]. The typical TVG of 40 log R is used to compensate for transmission losses a signal experiences with range, R. It is

changed to 20 log R to compensate for a sampling volume instead. Whilst these physical adjustments to the sonar can effectively implement the theory of echointegration [50], it may also be possible to use ML techniques to achieve the same outcome. By creating databases consisting of various density distributions, the scattering field effects of multiple targets may be modelled using aggregated digital signal data. Investigations are needed to test this methodology, as successful implementation may lead to computationally efficient modelling for valuable abundance data.

2.3. Evaluating Sonar Systems and Machine Learning Techniques

Although the models trained and tested on high-resolution images have shown high accuracy [51], the devices used are expensive. Farmers find any cost-benefit nullified when assessing the capital required against the potential savings from efficiency created. This presents the opportunity to achieve a similar outcome to previous studies using simpler sonar systems. The literature shows promising results for utilising simpler forms of acoustic technology to achieve effective target detection and biomass estimation. Kim et al. [52] successfully obtained TS information of redlip mullet fish by scanning 16 live fish with a split-beam echosounder. They measured their weight and lengths, thus providing them with the statistical relationships between the three values and producing equations to help estimate biomass. The study underlined the significance of obtaining TS parameters to obtain insights into the scanned environment and how numerical values of target strength and volume backscattering through echo-integration can provide the end user with a quantitative analysis of the observed species. Approaches like this can ultimately pave the way for cost-effective solutions for farmers to incorporate sustainable practices through intelligence-based systems [53], providing needed reliable data.

2.3.1. Comparing Acoustic Systems

Deploying simple active acoustics, whether single, dual, or split beam, presents challenges due to the necessity of steering the acoustic beam to cover a sample volume. In contrast, multibeam echo sounders capture coverage in one swath

using multiple beams, assessing different water columns at various angles [54]. To address this limitation, designers like OTAQ incorporate a stepper motor to sweep a defined area mechanically. While this method mimics an MBES operation, it necessitates a set interval to complete a full scan. Slow scanning speeds can be exposed in dynamic environments, where fast-moving targets may not be scanned adequately or at all, leading to reliability issues. The costs of mechanical elements, such as stepper motors, are comparable to those of additional electronics required for a phased array, which allows for electronic rotation [55]. Although a phased array system is more complex to design, its scanning speed is superior and less vulnerable to damage, resulting in lower maintenance needs. Passive acoustic systems [31], [56], [57] have also shown high promise in their implementation as part of automatic intelligent feeders for shrimp. The analysis of sound emitted by shrimp mandibles during feeding may offer a more reliable avenue of research if the pursuit of active acoustic solutions proves unsuccessful.

2.3.2. Machine Learning Techniques

Machine learning is the process through which machines are programmed to learn from past data to find patterns, insights and mathematical expressions to make judgements about future data [58]. Proposed methods generally follow the basic procedural framework as shown in Figure 4. Supervised ML methods can be tedious and time-consuming, particularly during the data acquisition and preparation stages, where data requires manual capture and labelling. Despite this, ML techniques are simple to implement in almost any application with any data format, making it an ideal basis for modelling low-resolution acoustic data.

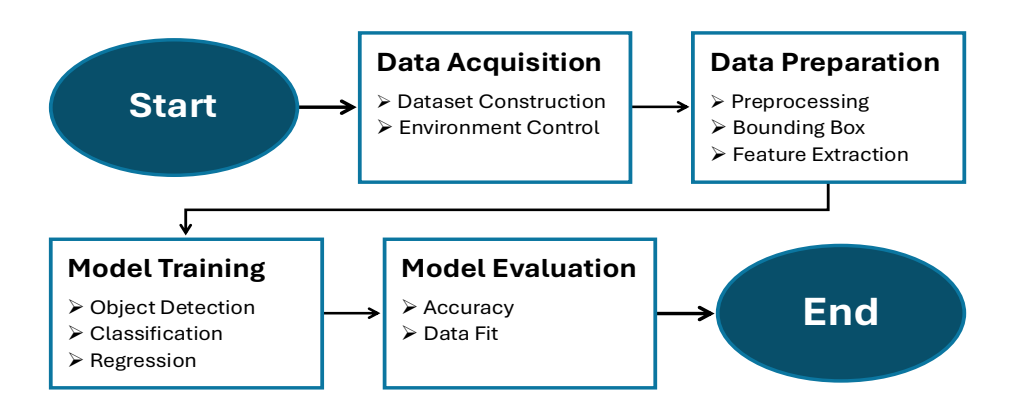


Figure 4 – General process flow for ML-based approaches

ML-based approaches have been broadly used in fishery acoustics in recent years, with ANNs, KNNs and RF algorithms finding success in their respective applications, summarised in Table 1 [59]. Another popular ML technique for interpreting echograms is the YOLO network. It is a convolutional neural network variation that can predict bounding boxes and classify targets at once. Lin et al. [21] successfully developed a YOLOv4 network that identified the number of white shrimps with 97.3% accuracy when varying the number of shrimps from 1 to 4 and their orientations.

Paper	Target	Acoustic System	ML Models	Accuracy
Minelli et	Fish School	MBES	KNN and	98%
al. [23]	and gas		boosting	
	seeps		ensemble	
Proud et	Rastrineobola	Multifrequency (70	Random forest	85.40%
al. [24]	Argentea	and 120 kHz) EK60		
	(dagaa)	Echosounder		
Villar et	Argentine	SIMRAD EK500	ANN models:	MLP:
al. [60]	anchovy,	echosounder	Multi-layer	97.99%
	Longtail hoki,		Perceptron	SOM:
	Blue whiting		(MLP), Self-	96.63%
			organising	
			Mapping	
			(SOM)	
Aronica	Anchovy,	Multifrequency (38	ANN models:	Multibinary:
et al. [61]	Sardine and	and 120 kHz) EK60	multibinary	88.20%
	Horse	and Probe	and multiclass	Multiclass:
	mackrel		neural	90.56%
			networks	

Table 1 – Key research using ML for fishery applications since 2018 [59]

These investigations confirm that ML is a viable approach for analysing marine species using sonar technology. Studies can build upon these works to propose additional methods that streamline data acquisition and processing times using commercially applicable DAQ systems.

2.3.3. Acoustic Data Acquisition

The consensus of scholars reviewing the development of ML techniques for biomass estimation is that the research is generally very limited [6], [16]. The lack of full-scale studies has resulted in a lack of analysis on proposed methods, with no single method being widely accepted and supported by sufficient testing. The stagnation in research progress is probably due to the challenges of conducting robust experiments, especially when machine learning techniques are involved. Chai et al. highlight the significant challenges in acquiring adequate sonar data and the lack of publicly available datasets as primary obstacles. The nature of constructing and labelling echogram datasets is time-consuming when considering the breadth and variety of data needed to train an effective classifier [16]. The paper reviews the DL in aquaculture, recommending a focus on building publicly available datasets to reduce data acquisition times. This would leave more time for data processing and developing digital solutions. Several studies have converged on the same area of exploration: the positive demonstration of applying DL classifiers to sonar data. However, investigations have lacked the scale to analyse the true benefits of these applications in aquaculture farms and how they compare to traditional manual methods. It is clear that the full potential of ML methods for precision aquaculture will not be realised until effective data collection methods have been thoroughly explored.

In recent years, several innovative solutions have been proposed to address data scarcity and slow acquisition rates. These have primarily originated from entirely different acquisition processes, such as using advanced simulation techniques with 3D models to rapidly generate synthetic data that mimics real sonar images. Sung et al. [62] developed a method that employs a Generative Adversarial Network (GAN) for scanning sonars, generating simulated data and comparing its realism to actual images. The team utilised ray tracing to emulate sonar imaging, modelling nonlinear phenomena by training a GAN with real sonar images. This approach captured features through a 15-layer U-Net, inducing realistic noise and degradation effects. The study demonstrates that techniques can rapidly generate

large synthetic image datasets, underscoring the potential to overcome environmental limitations in data processing tools.

2.3.4. Analysing Acoustic Shrimp Data

The procedure for processing hydroacoustic aquaculture data is generally consistent across marine species, but gathering the biological context for those being studied is crucial for fine-tuning solutions. Understanding shrimp's physiological, environmental, and behavioural patterns in production ponds enhances data quality extraction [57]. One of the biggest challenges in scanning decapods like shrimp, crabs, or crayfish is the lack of an air-filled cavity in their anatomy, unlike most fish. According to Foote [63], a swim bladder can dictate 90% of the backscattered signal, with the rest of the physiology of the fish seemingly invariant to any significant deviations to the energy reflected. But as Nakken et al., Elliot, and Kim point out, key fish characteristics, such as its size [64], length [52] and tilt [65], influence the shape of this swim bladder. TS is, therefore, used as a function to estimate fish biology, with its application yielding successful results. The swim bladder significantly influences fish acoustics due to its effectiveness as an acoustic reflector, with gas-filled cavities showing a notable impedance difference in the water medium. This results in characteristically high TS readings amongst the noise mask, making fish easily identifiable. Clear and prominent readings subsequently enable deep learning tools to extract features from the data better, simplifying ML tasks.

By contrast, the absence of a gas cavity means that decapods and shrimp are classed as weak scatterers [18], reflecting a weak signal that is often diffused in nature. The complexity in categorising swim-bladderless species of marine life has resulted in research aimed at accurately differentiating between various classes of zooplankton. The most important work in this area has arguably been done by Stanton, producing several papers classifying zooplankton into three anatomical categories [66]:

- 1. Fluid-like (copepods, shrimp-like or salps)
- 2. Elastic-shelled (gastropods)
- 3. Gas-bearing (siphonophores)

By ensonifying animals with a broad frequency spectrum, Stanton produced TSfrequency plots that are typically used for target identification [67]. Through a series of live and laboratory-controlled experiments, it was discovered that three distinct acoustic signatures could be observed and modelled for the three anatomical types of animals. This indicated that shrimp morphology produces a distinct and recognisable TS. Analysing the time differences of signal arrivals suggested that the acoustic pulses penetrate the body before echoing, indicating that the tissue of the shrimp contributes to the acoustic reading. This information provided the basis for the progression of more accurate scattering models. Research on shrimp scattering models surged after Stanton's work, focusing on accurately capturing sound scattering. Initially, sphere models represented shrimp volume, emphasising material but neglecting length and orientation. This gap led to cylindrical models better capturing the shrimp's shape. Subsequently, higher resolution models emerged, notably the Distorted Wave Born Approximation (DWBA) from Lavery et al. [68]. While these high-resolution models effectively predict individual shrimp backscatter, they are impractical for low-resolution imaging. For shrimp abundance using echo-averaging, simpler cylindrical models will likely suffice.

It is difficult to demonstrate the degree to which biological factors influence target strength when present simultaneously, as each factor cannot be easily examined in isolation. By evaluating the biological factors of 25 adult walleye pollock, Elliot et al. [63] found that tilt demonstrated a greater acoustic influence compared to length and depth, corroborating Foote's research that any target strength regression must account for tilt. Orientation may introduce unwanted transience in data, potentially leading to misleading conclusions, even for the most robust ML models. This makes the concept of producing definitive hydroacoustic insights into weaker signal targets appear impossible to achieve as a solitary observation tool. The subtext underlying the conclusions of these publications suggests that supplementary techniques relied upon by farmers, such as trawl sampling, must still be incorporated into any data modelling to validate the insights derived from the data. Ultimately, it signifies that hydroacoustic techniques, in their current

technological state, cannot yet be relied upon as automated solutions to replace existing methods of stock estimation, as even premium scientific equipment fails to provide definitive insights.

2.3.5. Financial Viability of Sonar Systems

To gauge the applicability of the proposed techniques, understanding the hardware used in this research direction is crucial. Studies primarily employ modern scientific MBES and imaging sonars for DL in aquaculture over basic single-beam systems. Devices of this specification produce echograms of high enough quality to easily apply DL techniques commonly associated with machine vision and optical images [54]. Scientific sonars significantly surpass uncalibrated devices in compatibility with hydroacoustic data processing programs. Software like Echoview derives measurements such as TS, enabling researchers to create statistical models alongside image classifiers to enhance accuracy. Whilst all these advantages point to the progression of research alongside scientific sonars, the field has so far failed to consider the financial feasibility of deploying these solutions in real-world applications for aquacultural farmers.

Scientific sonars are expensive. Multibeam sonars can cost over £2,000 [69], [70], with prices increasing significantly for advanced features and software. The current market prices out most farmers interested in incorporating new technologies into their current behaviour monitoring, feeding, sampling and harvesting operations. This is further exacerbated when considering the reduced profitability of farming small marine life, such as shrimp, compared to more valuable livestock, like salmon [25]. Working within a low-profit margin, local shrimp farmers, in particular, require a technical solution with a low capital cost and a potentially minimal subscription cost model to retain the technical support and services of a company such as OTAQ. The financial discourse surrounding the implementation of a solution for shrimp farmers suggests that research should prioritise the cheapest viable solution that maintains the ability to extract key data insights. The significant budget reduction must still provide a utility that comfortably offsets the expenditure required, whilst acknowledging that the hardware limitations will directly inhibit the performance of a potential solution.

Creating the most economical solution will lay a foundation that can be referenced to explore how incrementally improving the system's components by investing more capital can enhance data insights. Ultimately, the most optimal cost-to-performance ratio can then be pinpointed for deployment.

3. Methods and Materials

3.1. Operating Principles of the BRS-1

The sonar used in this study is the BRS-1 developed by OTAQ. The device is a horizontal single-beam scanning sonar that is mechanically driven. It consists of a 50 × 5mm rectangular transducer steered using a stepper motor with 400 steps. This allows the transducer to undertake 400 transmission-reception cycles at equal angular intervals across a 180-degree sweep. The transducer has an operating frequency of 640kHz, and a pulse is designed to propagate 5 metres. For every pulse-echo cycle, the received signal is filtered, amplified, and digitally converted into arbitrary intensity values scaling 0-4095. Range data bins are recorded 257 times, equidistant across the 5-metre range received. Further details of the sonar's hardware are found in Appendix 1. Once data is collected from one sweep, the string of intensity values is stored in a CSV log file and uploaded onto a Raspberry Pi network and cloud storage using an AWS S3 bucket.

3.2. Visualising Acoustic Data

Figure 5 depicts an echogram of the experimental setup, developed from the acoustic data of one sweep. The CSV format lets each intensity value be arranged in a grid describing its spatial information expressed in angle and range. Polar equations can be set up and converted into Cartesian form. Meshgrids add a dimension to the millimetre-scale spatial data, allowing 2 additional grids to be formed, aligning each data bin to its x and y coordinates. A contour plot expresses all the data, representing each bin as a pixel and using colour scaling to convey the intensity.

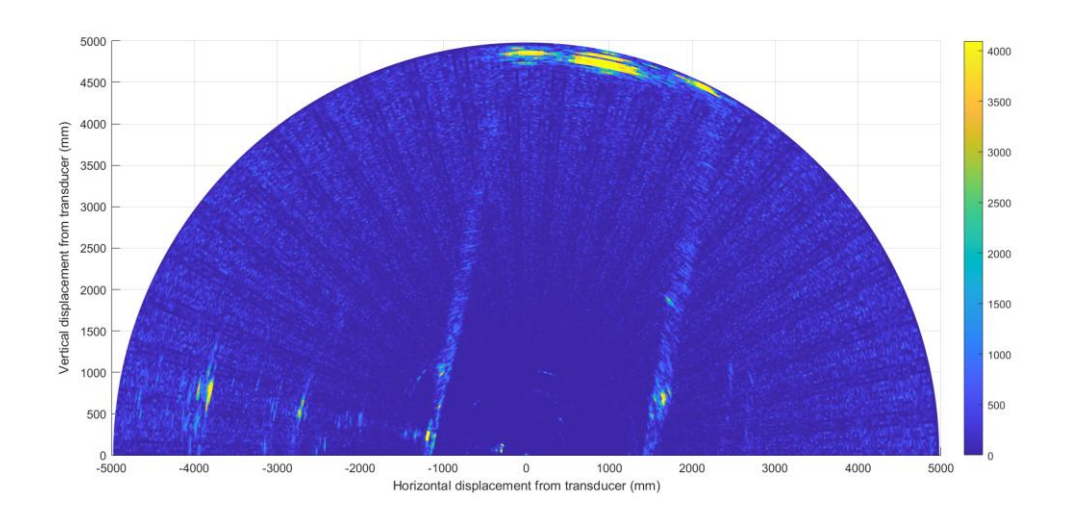


Figure 5 – Echogram of the tank used in the study created using data visualisation code

3.3. Method Process Flow

Experiments are carried out in a 2 × 5-metre water tank, filled to a depth of 1.5 metres with chlorinated water, as shown in Figure 6. The sonar was centred ahead of the rear tank wall and positioned at half the water depth. To investigate whether machine learning models can perform accurately using the BRS-1, this study follows similar procedures outlined by Kristmundsson [54], Zhang [71] and Pargi [22], involving data collection, data processing and modelling for analysis.

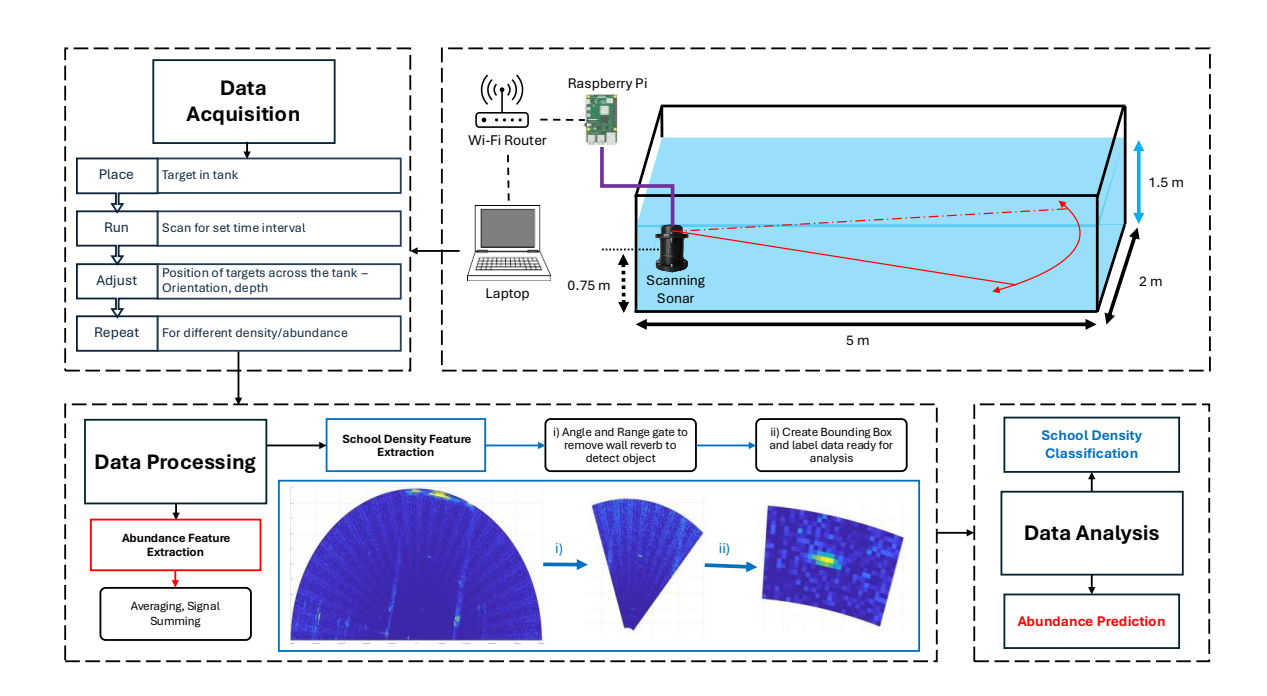


Figure 6 - Schematic of experiment design

3.4. Estimating School Density

3.4.1. Study Design

Dense schools can generally be received as singular echo traces by sonars [18]. Therefore, to model this, monofilament netting keeps targets together in a defined volume. School densities are formed by varying the number of targets in a monofilament wire net tethered to a sunk flat weight using a monofilament line to minimise reverberation [72]. A baseline for proving the concept with this device must be established. Hence, air-filled PVC spheres 55mm in diameter are used as targets to produce the most pronounced signal, shown in Figure 7. Spheres are isotropic reflectors [38], negating variables such as orientation. In practice, models true to field applications would need to be able to classify traces of schools in different positions and arrangements. For each quantity, the net is placed in different states such as its positions across the tank, at various depths, orientations and arrangements. For each state change, a scan is run, typically for 3 minutes, during which multiple sweeps of acoustic data are collected. In an initial run, 988 echograms are acquired, with at least 50 situations collected for each category.

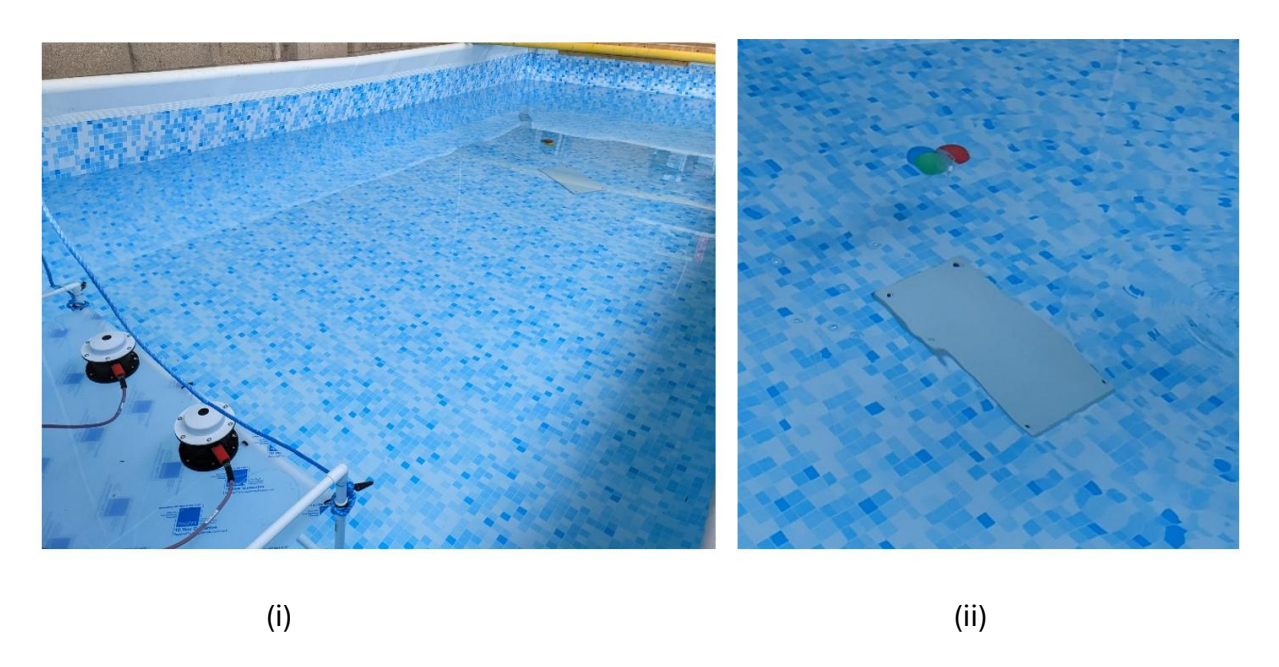


Figure 7 - (i) Experiment setup; (ii) Flat weight tethered to monofilament sphere bag

To increase the number of scans recorded, the sonar firmware is modified to reduce the size of sweeps collected at the acquisition stage using angle and range gating. By isolating the angular range to the 84 beams covering the effective area within the tank, which excludes wall echoes, 7.5 times as many sweeps are collected for any given time interval. This provides the opportunity to re-run the experiment with additional data to compare model performance between the two iterations.

3.4.2. Dataset Construction and Pre-Processing

In field environments, the features of a school trace should inform the user of the biomass contained within it, requiring data to correspond to a useful value. Labelling datasets with the desired information facilitates the categorisation of traces and the generation of useful model output. Hence, the data here is manually labelled after the number of spheres in the net, and we train classifiers to differentiate between the varying contents. A code is developed to search within the tank region for the echo trace within the scan. The detection function finds the echo trace and crops the sweep to isolate the region of interest from the background. Observational inspection discovers that a 21 × 31-pixel bounding box captures all the features of every trace acquired when centred around the highest-intensity pixel, demonstrated in Figure 8. Echograms are pre-processed using manual inspection to clean the dataset. The dataset is doubled through data augmentation by horizontally flipping the scans.

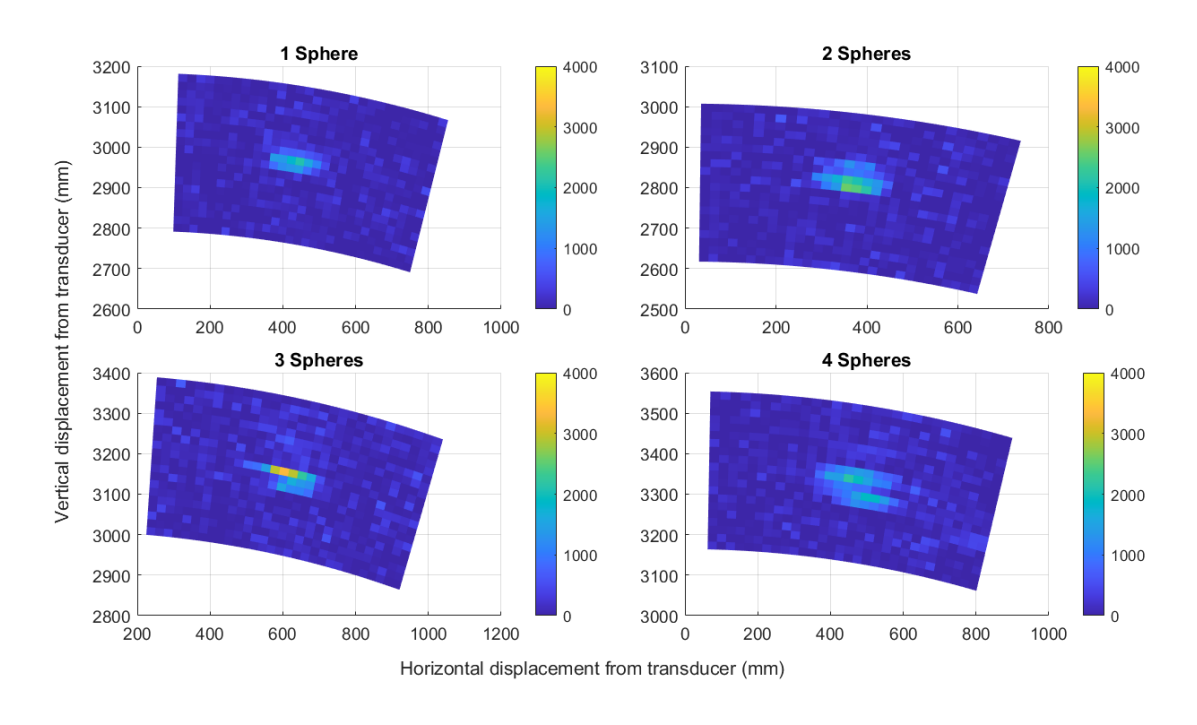


Figure 8 – Bounding boxes of variable-density echo signals used for model training

3.4.3. Data Analysis

Sufficient data is collected to analyse data using a 90/10 train-test split, where the 21 × 31 bounding boxes are input into models. Data is split randomly without predetermined segregation to ensure partitions are created without bias. Multiple classification models, including ANNs, RF algorithms, and support vector machines, are trained and tested in parallel to compare performance. Since bounding boxes contain pixels devoid of echo data, Principal Component Analysis (PCA) is employed to reduce feature selection, with a 90% preset used to explain data variance. Each model is optimised using Bayesian algorithms, where hyperparameters are systematically improved to minimise prediction error. The error is evaluated using 5-fold cross-validation to ensure models are generalised.

3.5. Estimating Abundance

3.5.1. Study Design

An artificial target is developed to investigate if low-cost sonar can produce interpretable data when scanning complex shapes, as would be the case in farming applications. The target approximating a shrimp is created by modelling its key features. Hydrogels are hydrophilic polymers used within the biomedical field to model the mechanics of soft tissues such as muscle and cartilage [73], [74]. This is applied to estimate shrimp's predominant soft tissue features using a bundled line of 3 hydrogel spheres, presented in Figure 9. This means that to create 80 targets, 240 spheres are submerged in water for 36 hours, growing from 5mm to around 30mm in diameter. They are wrapped in cellophane to allow bundling, where the excess wrapping is fed through a 10-millimetre hex nut before the whole target is coated in resin. This component represents the hard-shelled carapace. Shrimp are benthic feeders [21], [57]. Hence, the additional weight of a nut is incorporated into the model to allow targets to move with less restriction and stay biased to the bottom of the tank.



Figure 9 - Artificial target shrimp tethered to a wooden peg

Since flat weights would introduce a similar cumulative reverb signal, we did not see the incorporation of weight directly into the model as a significant issue.

Nevertheless, Figure 10 presents the findings for the 15 largest intensities in the

tank when scanning the acoustic model, a nut on its own, and when the tank is empty to quantify the hex nut's impact on the model. It is shown that the hex nut exhibits a very similar reading to the empty tank. In contrast, the target demonstrates an observable impact, indicating that signals received from the model shrimp are predominantly generated by the resin and gel features.

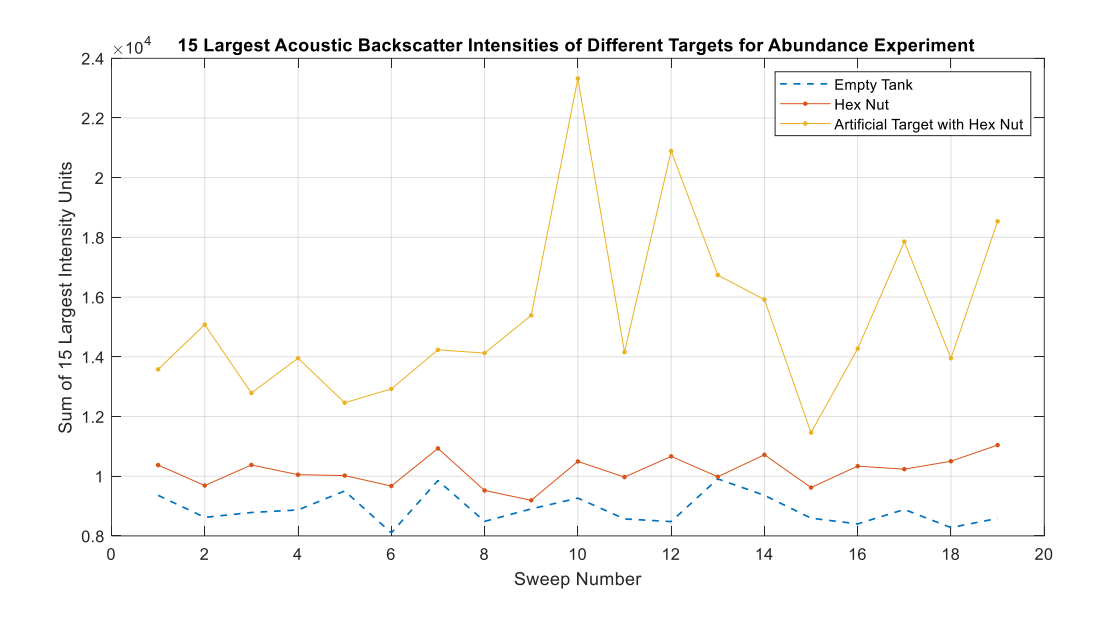


Figure 10 - Backscatter comparison of a hex nut and the final target

First, 80 targets are attached to clothes pegs with monofilament lines. Figure 11 shows a 3 × 2-metre pond-covering net placed over the back half of the tank.

Targets are suspended in the water by clipping the peg to the net through the mesh. Once a target is added to the tank, an angle and range-gated scan is run for 24 seconds, where 4-5 complete sweeps are collected. The state of the environment can be altered by manipulating the net plane. Tent pegs holding the net are reconfigured by stretching, slackening or repositioning the net to simulate the collective and controlled movement of the targets in all axes of freedom. Roughly 10 states are scanned for each target quantity. Stock can take up random spatial distributions and orientations. Hence, training data is varied using net movement to capture this and ensure models do not overfit. By suspending 80 targets within the 3 × 2-metre range, intensive stocking densities of shrimp are simulated, whilst smaller ranges represent intermittent and low cultures.



Figure 11 – Net overlay suspending artificial targets using wooden pegs and monofilament wire

3.5.2. Dataset Construction

The range and angle gating developed during the previous experiment means the scan covers 84 angles and 161 range bins to acquire tank readings. The dimensions of the data are reduced by summing the total intensity along each beam position, resulting in 84 features. Evaluating every pixel in a sweep can be computationally expensive and be a source of data overload [34]. Hence, employing echo-integration techniques like this simplifies the data, makes it easy to process, and prevents the need for additional equipment. Analysing large sections of sweep data can be challenging due to the high noise levels experienced in readings. Thus, denoising techniques are needed to clean the data. To increase the signal-to-noise ratio of each scan, all the available sweeps of the same state are averaged [18] to smooth out readings and reduce random noise whilst maintaining actual target signals. A code is built to extract the data from each scan folder and automatically provide label data based on the folder information.

3.5.3. Data Analysis

Due to this application's large number of discrete classes, a regression learning approach is opted for over classification. It is hypothesised that target number and summed intensity will be highly correlated, making regression learning models appropriate. In real-world shrimp farms, shrimp are farmed in ponds and can be stocked at different densities depending on the farming philosophy. While extensive cultures stock shrimp at approximately 1-10 shrimp/m², intensive cultures can stock shrimp at 25-30 shrimp/m²[9]. Thus, decision trees, random forest algorithms, neural networks, support vector machines and Gaussian Process Regression (GPR) models are trained with datasets of varying sizes and abundance ranges and compared to determine the ideal densities at which machine learning models perform. Evaluating ranges also investigates how overlapping echoes degrade data quality and hinder model performance. Bayesian optimisation algorithms are again used to fine-tune hyperparameters over 30 iterations to minimise the validation error of the 5-fold cross-validation.

4. Results

4.1. Estimating School Density

4.1.1. Evaluating Classifier Performance

Model performance is evaluated using performance metrics, including prediction accuracy, precision, recall, and F1-score, expressed as percentages, where a higher percentage indicates better performance. Since models undergo supervised training, accuracy is simply the percentage of correct positive and negative predictions from the total instances evaluated. Accuracy can be broken down further into precision and recall. Precision measures the correctness of positive predictions from the total positively predicted. Alternately, recall measures the proportion of true positives correctly classified as positive predictions. The F1-score measures the mean between the precision and recall [75]. Metrics are calculated using weighted macro averaging based on the number of instances in which each true class appears. This enables the evaluation of overall model performance while accounting for dataset imbalances.

Table 2 presents the performance found in unseen test data. It is observed that the best-performing model for this application is an optimised random forest algorithm that sampled 2 features using 481 trees with a maximum of 738 splits in a tree. Using 988 echograms from full sweeps resulted in an overall accuracy of 87.95%. The confusion matrix of the model shown in Figure 12 presents the distributions of predictions. A perfect model would demonstrate 100% true positives distributed along the leading diagonal of the chart. Deviations from the diagonal are represented as false negatives, which indicate misclassification. The matrix indicates that the overall accuracy is heavily biased towards the accuracy of detecting an empty scan, at 97.5%. The True Positive Rates (TPR) are inferior to the False Negative Rate (FNR) in classes 2 and 3, indicating that models were weak at distinguishing traces containing 2 or 3 spheres. The predictions made for 3-sphere echo traces being distributed comparably across all 4 target-present categories, which a low F1-score captures. Since 651 features are evaluated in each sweep, a

lack of data possibly hinders model performance. Without optimisation, data acquisition speeds are likely a limiting factor in obtaining the required data.

Model	Accuracy	Precision	Recall	F1
	(%)	(%)	(%)	(%)
Random Forest Algorithm	87.95	70.06	69.54	69.80
Single-Layer Neural Network	84.83	61.09	61.94	61.51
Single Tree	82.93	57.92	56.85	57.38
Support Vector Machine	84.72	60.99	61.42	61.20

Table 2 - Accuracies of models predicting sphere number

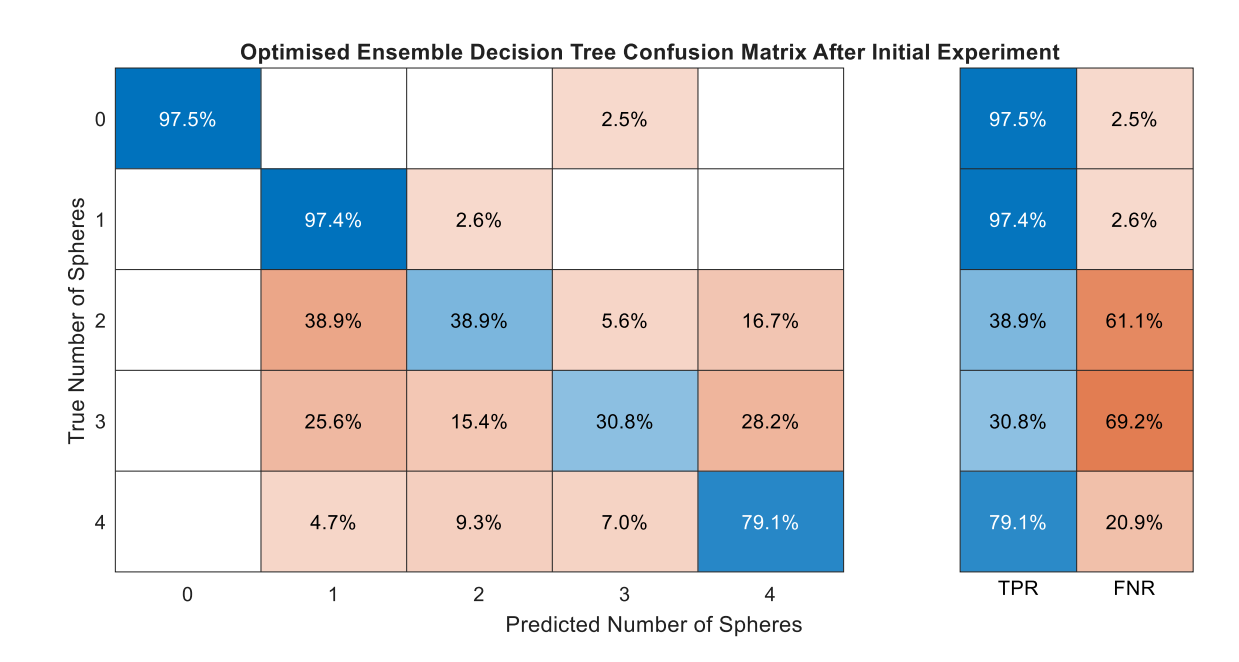


Figure 12 – Confusion matrix with true positive and false negative rates of the first iteration

4.1.2. Evaluating Performance using Data from Optimised Sonar

Using updated firmware, 2336 sweeps are collected, doubled through augmentation, and added to the existing dataset. For comparison, the performance of this iteration is evaluated in the same way as the previous experiment. Table 3 shows the performance improvement.

Model	Accuracy	Precision	Recall	F1
	(%)	(%)	(%)	(%)
Random Forest Algorithm	89.92	79.02	79.98	79.50
Single-Layer Neural Network	90.78	80.35	80.57	80.46
Single Tree	83.24	64.16	64.81	64.48
Support Vector Machine	89.32	77.52	77.71	77.61

Table 3 - Improved accuracies of models with additional data

Table 3 shows that the best-performing model was achieved using a Single-Layer Neural Network and a 90% PCA, with model accuracy improving to 90.78%. The network is optimised to have a 289-layer size with a Tanh activation function. The model perfectly predicts the presence and absence of targets in the tank, indicating that the model is well-suited for detection applications. Figure 13 indicates that significant improvements are seen across the leading diagonal in all classes, critically in classifying 2 and 3-sphere traces, which is reflected in the significant improvements in precision and recall. The TPR in each class is above 70% in every category. This suggests that increasing the dataset's size by an order of magnitude has provided the context to differentiate between echo traces more confidently. The error distribution generally stays between 1 class difference on either side, with errors beyond that accounting for a maximum FNR of 10% in each class.

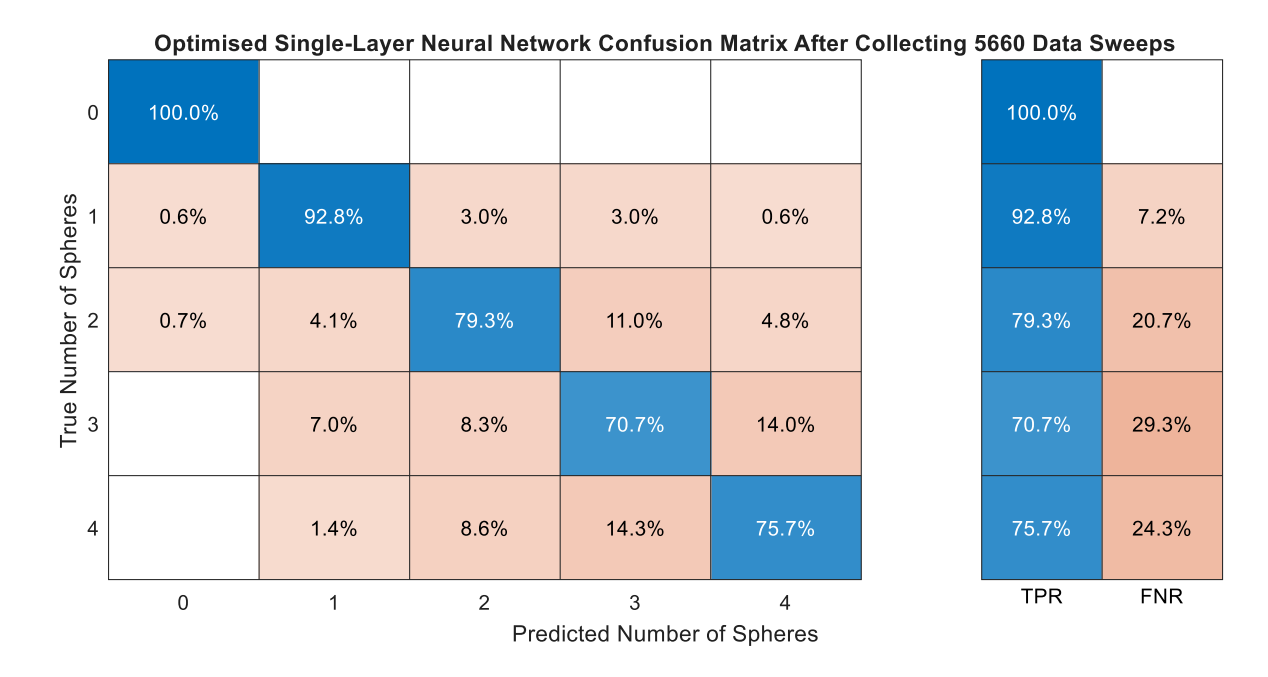


Figure 13 - Confusion matrix with true positive and false negative rates of the second iteration

4.2. Estimating Abundance

Evaluating Regression Model performance involves analysing prediction errors using the Mean Absolute Error (MAE) and the Root Mean Square Error (RMSE). The model's fit to test data is evaluated using the R-Square, where a value closer to 1 expresses a better fit. Table 4 summarises the performance of each trained model when trained on a complete dataset, predicting abundance from a target sample range of 80. Neural networks and GPR models are well-suited to this application, with GPR models demonstrating the best performance. Using a 90/10 train-test split, the model fits the data strongly. The R-squared value of the GPR model conveys its ability to explain around 98% of the variance in the test data. This is further depicted with test predictions being correctly predicted to an average error of 2.42 of the targets, around 3% of the sample range. Although the results reflect a controlled lab setting with static targets, anything short of a steep decline in performance from this baseline caused by noisy environments can still be viewed as a satisfactorily functioning model.

Model	MAE	RMSE	R-Squared
Random Forest Algorithm	4.23	5.76	0.937
Gaussian Process	2.42	3.24	0.980
K-Nearest Neighbour	4.86	7.29	0.900
Single Tree	4.48	6.94	0.908
Support Vector Machine	4.97	6.90	0.91
Three-Layer Neural Network	2.91	3.97	0.970

Table 4 – Performance metrics of abundance estimation models when trained on a full 80-target dataset

Model performance is further compared at different abundance ranges, as summarised in Table 5. The results validate the GPR's suitability for this application; it is the best-performing model in all but one size range. After increasing sample size testing by 10 targets at a time, it is clear that regression models predict abundance best when the maximum number of targets is 50 within the 4 m² sample area, equating to a 12.5 target/m² density.

Abundance Sample Range	Best Performing Model	MAE	Maximum Residual as a Percentage of Abundance Range	R- Squared
0-40	Gaussian Process	1.33	14.15 %	0.979
0-45	Gaussian Process	1.62	12.6 %	0.979
0-50	Gaussian Process	1.36	6.8 %	0.989
0-55	Gaussian Process	1.58	8.8 %	0.985
0-60	Gaussian Process	1.90	10.3 %	0.982
0-70	Random Forest Algorithm	2.33	11.1 %	0.978
0-80	Gaussian Process	2.42	12.5 %	0.980

Table 5 – Performance metrics of the best models created when training and testing on different abundance sample sizes

Further sample sizes are tested at more precise intervals around 50 to observe potentially more optimal ranges; however, the additional data confirms that range 50 has the lowest error. The data also aligns with the strongly correlated pattern in model performance with range. At conservative ranges, models seem to observe competitive absolute errors. However, the models are normalised for better

comparison by finding the percentage error of the biggest residuals for each model. As a result, these low-range models are found to predict relatively high error values, which is reflected in their inferior ability to explain variance, expressed by a lower R-squared value. This is likely due to the smaller dataset size resulting from limiting the abundance sample. It may be found that if models were trained on equal-size datasets, conservative-range models would match, if not outperform, the best model with the added context. In contrast, models operating with higher abundances increase in error with abundance after the optimal range. This aligns with expectations due to the deteriorating effect of increased stock density on a signal passing through it [54]. Increasing the density reduces the differences in the total acoustic energy received between 2 consecutive target quantities. This makes prediction variance challenging to explain for data that is progressively similar. Figure 14 displays the distribution of residuals for the GPR trained on an abundance range of 50. Residuals show no sign of correlation, indicating well-balanced and robust performance when predicting scans of unseen states.

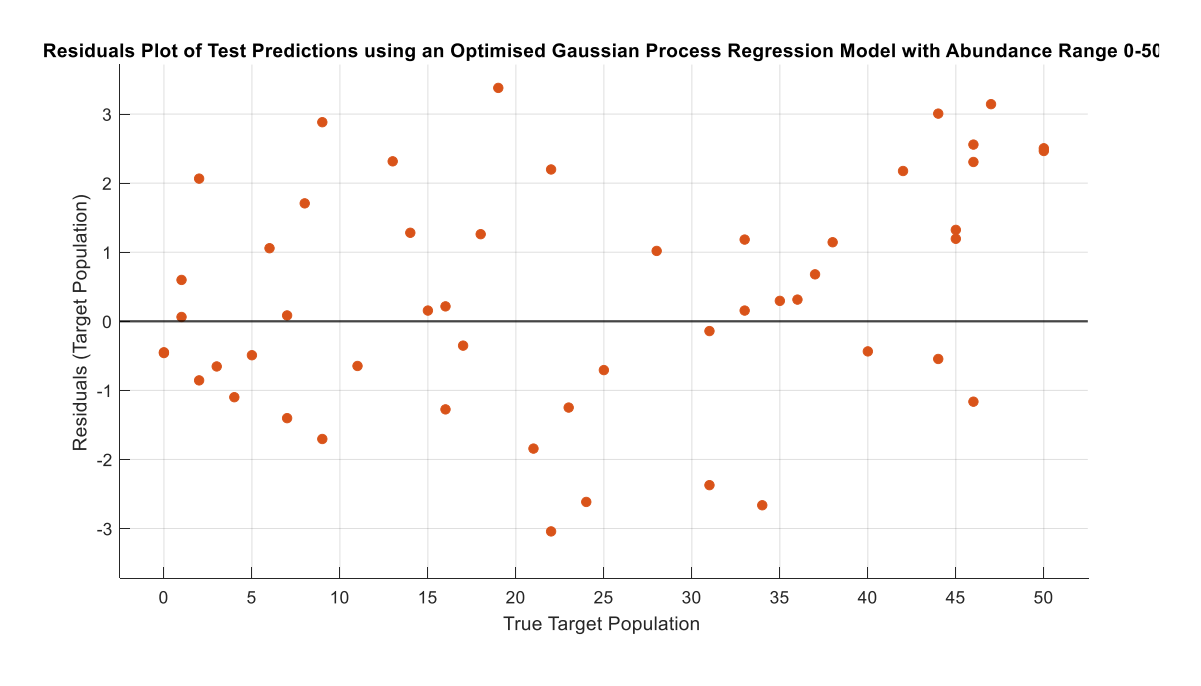


Figure 14 – Residual plot when tested on a 50-target density

5. Discussion

Our results demonstrate the success of machine learning in interpreting and explaining low-resolution 2D acoustic data for abundance estimation. Using a variation of echo-integration, we show that regression models can fit to scan data with an R-squared of 0.989 even when data dimensions are reduced, exploiting a computationally efficient data processing method and achieving predictions accurate within an error of 1.5 targets. A technique has effectively detected objects and automatically processed them into the appropriate structure for analysis. ML classifiers can categorise echo traces into density information to an accuracy of 90.78%, establishing a baseline of feasibility for classification applications.

Modelling density using a net full of hollow uniform spheres introduces the concept to sonar and ML methods at a rudimentary level. Using simple targets here creates a simplified and idealised representation of school densities. As such, results reveal the potential limitations for commercial implementation. Airfilled spheres backscatter noticeable acoustic energy due to the high acoustic impedance differential between air and water. This makes signal changes more pronounced, creating differences in data that are seemingly easier to classify for ML models. With this context, an F1-score of 80.46% suggests the sonar is not currently suited to reliably classify densities of more complex and weak backscattering shrimp targets in this manner. This can be explained through several technical aspects: (i) Low resolution, particularly in the range where echo data is resolved at around 20mm, making it possible for crucial echo data to be skipped over. (ii) The lack of spatial information in the z-plane makes sphere arrangements challenging to interpret. (iii) Horizontal propagation relies heavily on reflection angles to carry echo data [47]. The transducer size can be deemed suboptimal for this application, with a narrower beam reducing the number of reflections, which is likely to yield more precise data. (iv) High noise introduced predominantly by signal processing and electroacoustic circuitry. This creates speckle noise [16] amplified with the range due to the time-varied gain amplifier, degrading data quality even in laboratory conditions. Although these hardware

limitations render the sonar incapable of serving as a scientific measuring tool, the device is found to be coherent enough to have its data interpreted using ML techniques. However, limitations that create such noise and low resolution make analysing individual echo signals through bounding boxes challenging, simply because of the lack of information conveyed by the sonar within the regions of interest. Breaking down compact overlapping echoes within cropped sample areas to estimate individual school density is therefore a suboptimal application for this specification of sonar.

In contrast, utilising a larger portion of the sonar's observational capacity for general abundance estimation shows greater compatible functionality. Regression models estimating abundance demonstrate a correlation between increasing sample range and absolute error, maintaining a maximum percentage error of around 10%. Increasing training data in more diverse positions may enhance accuracy in explanations of these variances [54]. Whilst a recommended maximum abundance has been found, sample sizes both greater and smaller can have data variance explained to a similar standard. Despite this, some limitations must be considered. For abundance estimation, the data processing method employs averaging, an effective technique for enhancing the signal-to-noise ratio. However, this can only be executed reliably in static conditions where targets remain still during scanning, which is improbable during in situ observations, where averaging may be misrepresentative [6]. It may be possible to sweep faster with improved hardware and to take minimal sweeps, achieving the same effect before major movements occur within a few seconds. While training time and computational speeds are realised in real-world applications, they are not considered factors in this study. Nevertheless, the study uses an 8th Gen Core i5 processor, available on easily accessible hardware, to develop each model. Hardware limitations can become apparent when training GPR models on range-80 data that is augmented to double in size. The exclusion of the augmentation step from the experiment still produces satisfactory results, with its inclusion unlikely to significantly enhance models based on the results.

Using a basic cost-effective specification, the sonar produces data that can be used to make population predictions in a sample area. Whilst it is not determined how closely the artificial targets approximate shrimp, the rough, heterogeneous nature of the targets means real-world parameters such as orientation, depth and material can be captured to a reliable degree in a varied dataset to make accurate predictions. The effect of the abundance range impacting predictions is correctly observed. Placing a proportion of targets on the tank floor to simulate shrimp behaviour is data that models can explain to a reasonably good standard. The targets may better represent alternate stock with greater reflectivity, such as fish [65], in which case, results can still serve as a helpful reference. To more closely simulate field conditions, such as using real shrimp, is beyond the scope of this study, yet from these constraints, creative modelling methods are proposed to overcome the challenge of sonar data acquisition.

Expanding on artificial target modelling can form the basis of reframing future studies to overcome the obstacles of on-field data acquisition. The results serve as a marker of capability for basic specification sonars. Despite their compromise on hardware components, regression models can interpret the acoustic data of well-balanced datasets to make accurate predictions.

6. Conclusion and Recommendations

This project utilises a basic specification scanning sonar to collect training datasets of two circumstances applicable to a shrimp farming environment. Developing a visualisation tool helps process data and create further automated tools for feature engineering tasks. Whilst the sonar is hardware-limited to break down the details of an echo trace, angle-gating scans offer the data acquisition speeds needed to produce reasonable classification accuracies. Echo-integration strategies heavily reduce the features required for prediction and allow regression models to interpret sweep data effectively, mapping data to an R-squared of 0.989. Models can predict the population between 0-80 targets to a mean absolute error of 2.3, indicating a methodology is presented whereby insights can be derived from basic acoustic data. It also suggests that sonars of this specification can be incrementally improved upon to be deployed in real shrimp ponds as an affordable solution.

It is recommended that artificial target models be refined for shrimp for easy testing to overcome health and safety regulations in laboratory environments. Sonar specifications may additionally be improved upon to observe how improvements in hardware correspond to model performance against cost. Datasets should be collected in real pond environments to investigate how environmental factors impact acoustic propagation and data quality.

Appendices

Appendix 1 – Hardware Features of OTAQ's BRS-1

The BRS-1 is an acoustic telemetry system designed and manufactured by OTAQ to function as an active-pulsed sonar designed to detect shrimp within a submerged body of water. Short for Biomass Reader for Shrimp, the device is integrated into an Internet of Things (IoT) infrastructure, whereby digital data is generated from electrical signals induced within the receiver electronics. The hardware components are operated by a Raspberry Pi controller, which sends command prompts to the device via its network. The generated data is stored in log files. The raw data can be post-processed into several forms for analysis, with the aim of creating valuable insights for farmers, such as the behaviour of shrimp or the biological morphology index of shrimp, including biomass, length, and population within a sampled area.

The system can be broken down into 3 components, interworking to facilitate a robust and cost-effective solution:

- The BRS-1 Hardware: The transducer, stepper motor and associated circuitry.
- 2. The Raspberry Pi network and Firmware: Digital signal data generation and storage.
- 3. Post-Processing Software: Code to transform data for digitalisation and machine learning.

The post-processing software is the primary focus of the research project, and the network features of the system utilise protocols common for IoT and cloud storage solutions. Hence, this appendix will detail the hardware components featured in the BRS-1.

The BRS-1's hardware can be segmented into four categories:

- The Central Processing Unit (CPU)
- The stepper motor and drive electronics
- The transducer, connected to the transmitter and receiver electronics

• An Inertial Measurement Unit (IMU)

The Main Printed Circuit Board (PCB) facilitates connection points between the CPU and all other components. Therefore, the device's firmware, which contains the operational instructions of the default function, is uploaded onto the CPU via a Power over Ethernet (PoE) cable. The PCB also includes a Serial Wire Debugging (SWD) port, which allows external devices to communicate with the device and facilitate debugging. SWDIO (Serial Wire Debugging Input/Output), SWCLK (Serial Wire Clock), and nRST are pins available within the device to enable the execution of protocols for handling malfunctioning devices. The CPU consists of two STM32 processors, one of which is dedicated to managing the power supply. A 2980 stepper driver is used to power the stepper motor, relay the sweep instructions, and evaluate the current step position of the motor.

Using two MOSFET switches, the transmitter produces a square wave signal at the operating acoustic frequency of the transducer (64 kHz). Capacitors are integrated into the circuit to smooth the wave's rise and fall times, thereby enhancing consistency. To handle the high frequencies and the necessary high voltage, the MOSFET switches are paired with drivers. The primary benefit of using MOSFET drivers in the sonar system is enabling high switching speeds while minimising switching losses. These drivers supply the required voltage to surpass the high gate threshold voltage, enabling the MOSFET to switch on and allowing the higher source voltage to be delivered to the transducer, as shown in Figure 15. The low impedance of the driver Integrated Circuit (IC) ensures that the gate capacitors are charged more quickly with the correct voltage and discharged faster through a lower resistance pathway provided by the driver, resulting in faster switching. This also helps protect the MOSFET from overheating and high-voltage damage by reducing the effects of the gate capacitance and inductance. The microcontroller, which provides the low-voltage square wave, is protected from potential back current due to the driver's resilience to negative transients travelling from the transducer through to the drain. When the transmitted square wave signal matches the natural frequency of the transducer, resonance is achieved, resulting

in increased stresses and strains within the piezoelectric material, which induces amplified vibrational amplitudes at the same frequency [37].

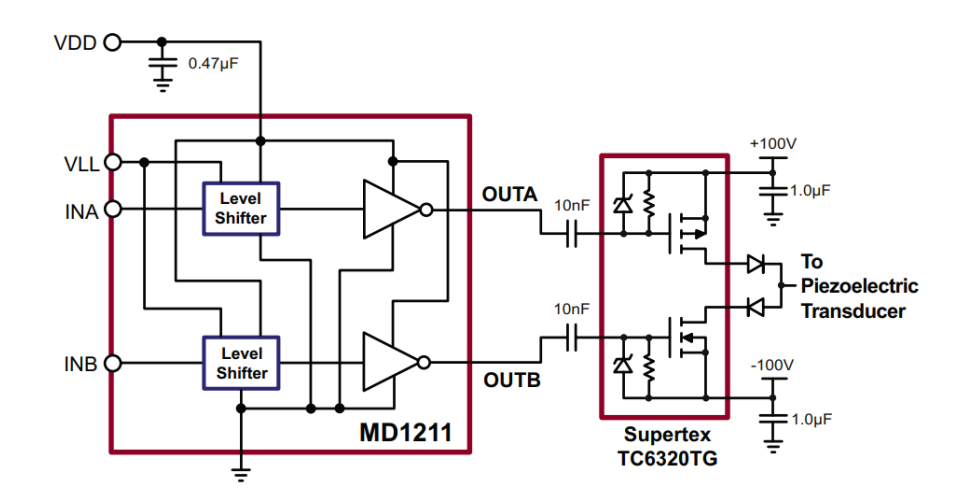


Figure 15 – Schematic of MOSFET and driver circuit [76]

Comparatively, the receiver electronics are more complex, requiring a differential amplifier, fixed and TVG components, and Butterworth filter. Each component is vital in the signal-treating process, eliminating noise and amplifying the signal for digital conversion and analysis. A TVG signal is created digitally to compensate for the transmission losses that accumulate with distance. This signal is fed through a Digital-to-Analogue converter (DAC) using a bandgap voltage reference to maintain the signal's precision with a stable step voltage and resolution. A timer within the microcontroller is programmed to supply the variable gain following the exponential TVG range function of 40 log R. The gain is varied using a Lookup Table (LUT) instead of external Programmable Logic Devices (PLDs). While PLD microchips use an integrated circuit of logic gates to execute continuous functions, LUTs are tabular data structures containing two sets of pre-computed values [77]. This means the LUT applies pre-assigned gain values to a discrete number of time intervals to mimic the 40 log R function. Implementing LUTs using the microcontroller frees the CPU from performing computations by running simple data search and retrieval protocols, making the device more efficient in terms of space, expense, and computational cost. However, the efficiency from a discrete number of lookup values compromises the smoothness of the signal, as only a finite number of gain values are applied rather than the ideal gain curve. The device also compromises on responsiveness due to a microcontroller that is

overstretched in managing multiple systems within the device. While PLDs can perform calculations in nanoseconds, relying on the microcontroller to run retrieval protocols can still take microseconds to perform. The TVG signal is input into the receiver filter alongside the true received signal, with a signal derivative of both being fed through using another operational amplifier generated by the transducer from the echo signals. The received signal must only contain frequencies close to the original pulse projected to confirm it is from the echo signal and reject reverb and unwanted noise from the scanned environment. An active RC Bandpass filter ensures only the desired frequency range from the received signal is carried through for digital processing. The Butterworth configuration is used for this application, which prevents ripples or distortions from both the pass and stop bands, maintaining the accuracy of the echo signals. A gradual roll-off from the pass band allows any echo signal distorted from interfacing with a target to be picked up in the received signal at a reduced magnitude. The signal is subjected to further amplification using a closed-loop gain design, leading to a controlled and reliable increase in the signal magnitude and smoothing. The valuable data in the echo signal is the amplitude of the several peaks correlating to the acoustic reflectivity of the interacted targets. A rectifier circuit is inserted before the signal is digitised to isolate this data from the received signal. A series of diodes causes the carrier component of the signal to be removed, leaving behind an envelope signal. This processed signal is fed back into the main CPU microcontroller, which is digitalised for numerical conversions of signal amplitude for set intervals dictated by the CPU clock. The microcontroller that processes the signal has a maximum input voltage of 3 volts; hence, a Zener diode regulates the voltage by providing a back current path, preventing excess voltage being supplied to the input that can overload or damage the CPU. The voltage cap means the maximum digital signal received translates to a value of 4095, whilst a null reading outputs a zero. The raw numerical strings are sent to the Raspberry Pi network and formatted into log files.

An Inertial Measurement Unit (IMU) is a system integrated into each device, with the primary purpose of measuring and recording its relative orientation. In normal operation, the device is expected to be submerged upright, with the transducer face perpendicular to the water surface. The configuration ensures the device is running as a horizontal propagation sonar, with the echo data heavily influenced by changes in the elevation angle of the beam. The IMU's inclusion in the device provides additional telemetry to validate data and analyse orientation as a potential cause of anomalous readings. The hardware and firmware components had already been developed and well-integrated by OTAQ; however, a lack of post-processing analysis software maintained uncertainty regarding the feasibility of achieving a solution with the device in its current form. The lack of exploration here formed the basis of the project's overarching research question: Can post-processing data techniques be applied to the sonar's output to achieve valuable insights?

Appendix 2 - Sonar Visualisation Code

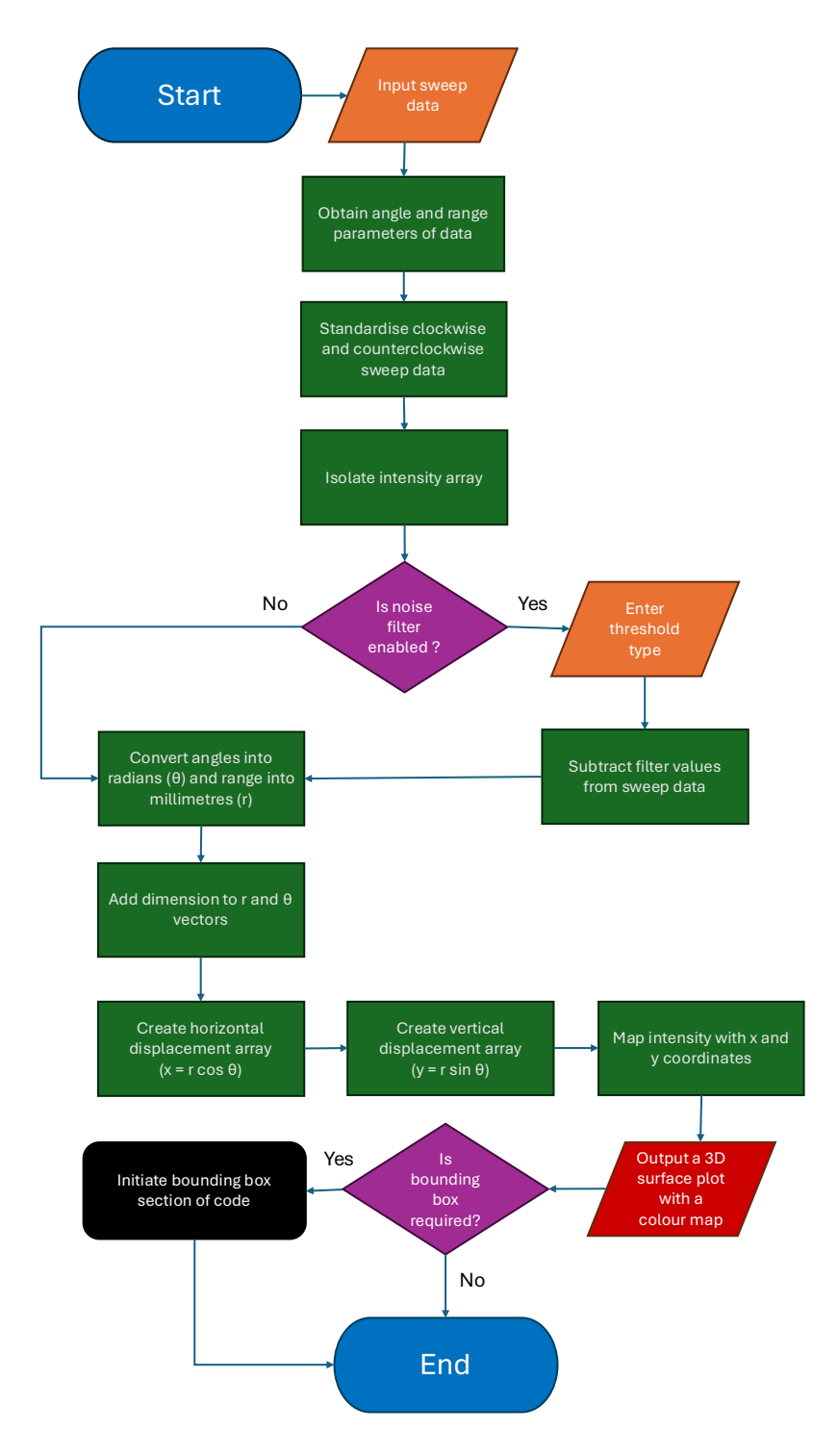


Figure 16 - Sonar data visualisation code flowchart

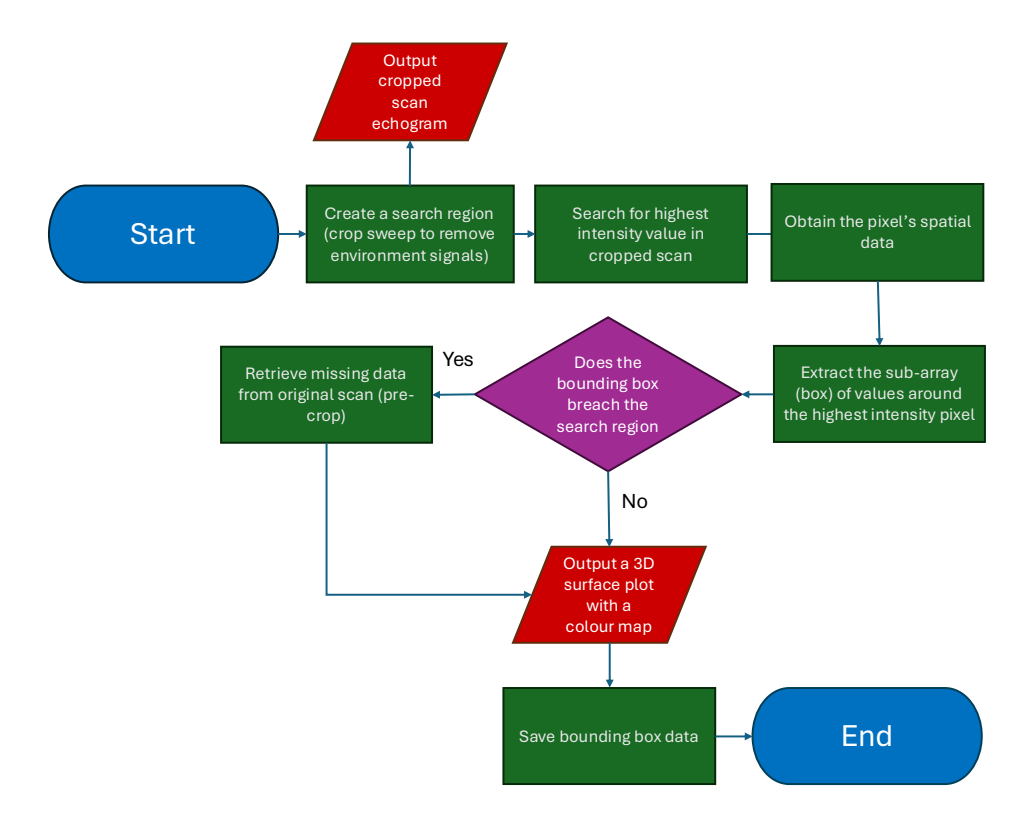


Figure 17 - Sonar data bounding box code flowchart

Code:

```
% sonar v3.4: Image, Bounding Box and if statement streamline
% v_.4: Bounding box multi-breach patch, Max value auto data tip
% -----
% - Description: This code visualises Sonar data output from the BRS by
% producing surface plots using a cartesian meshgrid to form Sonar Images
% - Code also creates sleuth regions and bounding boxes
% -----
% - Author: B.Eng. Hamzah Isap
% - Contact: hamzahisap02@gmail.com
% - Date: November 2024
function s = sonar(In,Bg,Av,varargin)
   % In: Sweep Intensity Array, Bg: Background filter toggle (optional), Av:
Background arrays needing averaging (optional)
  Sweepsize = size(In(:,:,1),1); wide = Sweepsize/2;
  offset = 0; minrng = 0; % Values are manually input based on parameters
chosen in the command window for the scan (fware: offset:-20,minrng:60)
  centre = 400 + offset;
  Angle = centre-wide:centre+wide-1;
  if In(2) == In(1)+1 % Default all sweeps to descend in angle
  In = flip(In, 1);
  end
  cIn = In(1:size(In,1),2:size(In,2)); % Crop 'In' (to make cIn) to remove
angle to only leave intensity
   if nargin == 1
       DeNoise = zeros(size(cIn,1),size(cIn,2));
   elseif strcmp(Bg,'none') % Type 2nd argument as none for no noise filter
       DeNoise = zeros(size(cIn,1),size(cIn,2));
```

```
elseif strcmp(Bg, 'average') % Type 2nd arg as average to use the 'Av'
input
       DeNoise = NoiseAv(Av);
       DeNoise = DeNoise(:,2:size(In,2));
   elseif isscalar(Bg)==1 % For a constant threshold, input a single numeric
value
       DeNoise = Bg.*ones(size(cIn,1),size(cIn,2));
   elseif isa(Bg, 'double')==1 % To subtract an already averaged or specific
       DeNoise = Bg(:,2:257);
   end
   cIn = cIn - DeNoise; % Denoise the scan
   cIn(cIn < 0) = 0;
   RngRes = 19.53125; % Range resolution / mm
   Dis = (RngRes*(minrng)):RngRes:(RngRes*(size(cIn,2)+minrng)-2); % Define
Distance
   th = 200.*ones(1,size(In,1)); % (Change dimensions column from the data
or a generated row array)
   Rad = (Angle - th).*(60/133).*pi/180; % Angular Resolution
   [rr, tr] = meshgrid(Dis, Rad);
   o = size(rr);
   x = rr.*cos(tr); % Convert to Cartesian coordinate system
   y = rr.*sin(tr);
   a1 = 1; a2 = 400; g1 = 15; g2 = 241; %centre: 175
   % Zoom Parameters z-(Angle range, Distance Range) - optional tool for
manual inspection
   %zx = x(a1:a2,g1:g2);
   %zy = y(a1:a2,g1:g2); % Carnforth Zoom (165:235,90:150) Carnforth Gating
~10 degree offset (185:265,1:230)
   %zIn = cIn(a1:a2,g1:g2); % Minnowtech Zoom (1:400, 26:60)
   p = surf(x,y,cIn); % Make z(vars) = R(vars) to see what area the bounding
box search is evaluating
       %surf for z values, p colour for just 2d images (x,y,cIn for whole
sweep)
   shading("flat"); set(p, 'Edgecolor', 'none'); colormap("parula");
colorbar % graphics options
   view(2) % View over the xy plane
   %clim([0, 4100]); % set manual colour scale instead of automatic ranging
 xlim([-5000, 5000]); ylim([0, 5000]) % set x-y scale (optional)
   pbaspect([2 1 1]) % Aspect ratio for angle and range gate within tank
   [mximus indxicus] = max(cIn, [], 'all'); % ID and locate the max-
intensity pixel of the scan (used for patched sonar)
   sciz = size(cIn);
   [row, col] = ind2sub(sciz,indxicus);
   locax = x(row, col);
   locay = y(row,col);
   locai = cIn(row,col);
   %datatip(p,locax,locay);
   %}
   -----%
   % This section of the code was used before the latest Sonar patch. Is
   % used to angle and range gate to create a sleuth region that isolates
the scan from the tank walls
   %
   if size(cIn,1) > 399
```

```
b1 = 110; b2 = 240; l1 = 20; l2 = 237; % b_ = angle limits % l_ =
range limits
   else
       b1 = 20; b2 = size(cIn,1)-20; l1 = 15; l2 = size(cIn,2) - 15;
   end
   % region of search scan
   Rgx = x(b1:b2, l1:l2);
   Rgy = y(b1:b2, l1:l2);
   RgI = cIn(b1:b2,11:12);
   %
figure
   ps = surf(Rgx,Rgy,RgI); % Outputs echogram of the sleuth region
   shading("flat"); set(ps, 'Edgecolor', 'none'); colormap("parula")
   colorbar; view(2)
   xlim([-5000 5000]); ylim([0 5000]); pbaspect([2 1 1]);
   %}
   %% ------%%
   % This section of the code creates a bounding box surrounding the
   % signal of interest which is the largest pixel in the sleuth region
   %
   [mx, is] = max(RgI,[],'all'); %Find the pixel in the gated scan that has
the largest intensity
   sz = size(RgI);
   %sprintf("RgI = %f", sz)
    [rw, cl] = ind2sub(sz,is); % Obtain the row (angle) and column (length)
number within scanned region of this pixel
figure % Create new image of bounding box of the ROI
   locx = Rgx(rw,cl);
   locy = Rgy(rw,cl);
    sprintf("max value in scan: %f \nlocation of max in x: %f mm\nlocation
of max in y: %f mm", mx,locx, locy)
    sprintf("row value: %d \ncolumn value: %d",rw,cl)
   w = 15; le = 10; slce = 0; shft = 0; % w: horizontal distance from centre
pixel and box edge, le: vertical distance;
    % This series of if statements are used if the centre pixel creates a
    % bounding box whose edges extend out of the sleuth region causing
    % missing data.
    % The statements recalls the missing data from the initial scan and
    % adds it on to complete the box
    % (Believe there is a much easier way of acheiving this by evaluating
the initial scan instead)
   if rw <= w %i.e 15</pre>
       slce = -(w-rw+1);
       sprintf("slce is: %d",slce)
       Rgx = [x((b1+rw-w-1):b1-1, l1:l2); Rgx(1:(size(Rgx,1)+slce),:)]; Rgy
= [y((b1+rw-w-1):b1-1, 11:12) ; Rgy(1:(size(Rgy,1)+slce),:)]; RgI =
[cIn((b1+rw-w-1):b1-1, l1:l2); RgI(1:(size(RgI,1)+slce),:)];
       %rw = w+1;
   end
   if rw >= b2 - b1 - w % i.e. 115 %'+2' taking into consider that e.g 4:10
is 1 greater than 10-4 and also here, we start with the row after that number
       slce = rw-(b2-b1-w)+2; %When the max pixel breaches both limits, the
new Rg must be cut and added to equally to ensure it can be contacated again
for the second limit
```

```
sprintf("slce is: %d",slce) % slce is the amount exceeded and this
how much should be taken off the top to be given to the bottom. It also comes
into play for correcting a second limit scenario
                  Rgx = [Rgx(slce:(size(Rgx,1)),:); x(b2+1:(b1+rw+w+1), l1:l2)]; Rgy =
[Rgy(slce:(size(Rgy,1)),:); y(b2+1:(b1+rw+w+1), 11:12)]; RgI =
[RgI(slce:(size(RgI,1)),:); cIn(b2+1:(b1+rw+w+1), l1:l2)];
                  %rw = b2 - b1 - w;
         end
         if slce < 0</pre>
                  shft = slce;
         end
         if slce > 0
                  shft = slce - 1;
         if cl <= le %if column number is less than the lower half-height of box
                  Rgx = [x(b1+shft:b2+shft, (l1+cl-le-1):l1-1) Rgx]; Rgy =
[y(b1+shft:b2+shft, (l1+cl-le-1):l1-1) Rgy]; RgI = [cIn(b1+shft:b2+shft, (l1+cl-le-1):l1-1) Rgy]; RgI = [cIn(b1+shft, (l1+cl-le-1):l1-1) Rgy];
(l1+cl-le-1):l1-1) RgI];
                  %c1 = le+1;
         end
         if cl >= 12 - 11 - le % i.e. 210
                  Rgx = [Rgx \ x(b1+shft:b2+shft, 12+1:(11+c1+le+1))]; Rgy = [Rgy]
12+1:(11+c1+le+1))];
                  %c1 = 12 - 11-le;
         end
         [rw, cl] = find(RgI == mx); %Re-evaluate rw and cl values
           sprintf("row value: %d \ncolumn value: %d",rw,cl)
         bx = Rgx(rw-w:rw+w,cl-le:cl+le); % Index the bounding box with the
largest pixel value at the centre
         by = Rgy(rw-w:rw+w,cl-le:cl+le);
         bIn = RgI(rw-w:rw+w,cl-le:cl+le);
         pb = surf(bx,by,bIn);
         shading("flat"); set(pb, 'Edgecolor', 'none'); colormap("parula");
%clim([0 2500]);
         view(2); pbaspect([1.5 1 1]); colorbar
         bIn = reshape(bIn, 1, ((2*w)+1)*((2*le)+1));
         bdata = [bIn locx locy];
         s = bdata; % Output the bounding box matrix
         %}
end
```

Appendix 3 – Echogram Timelapse Code

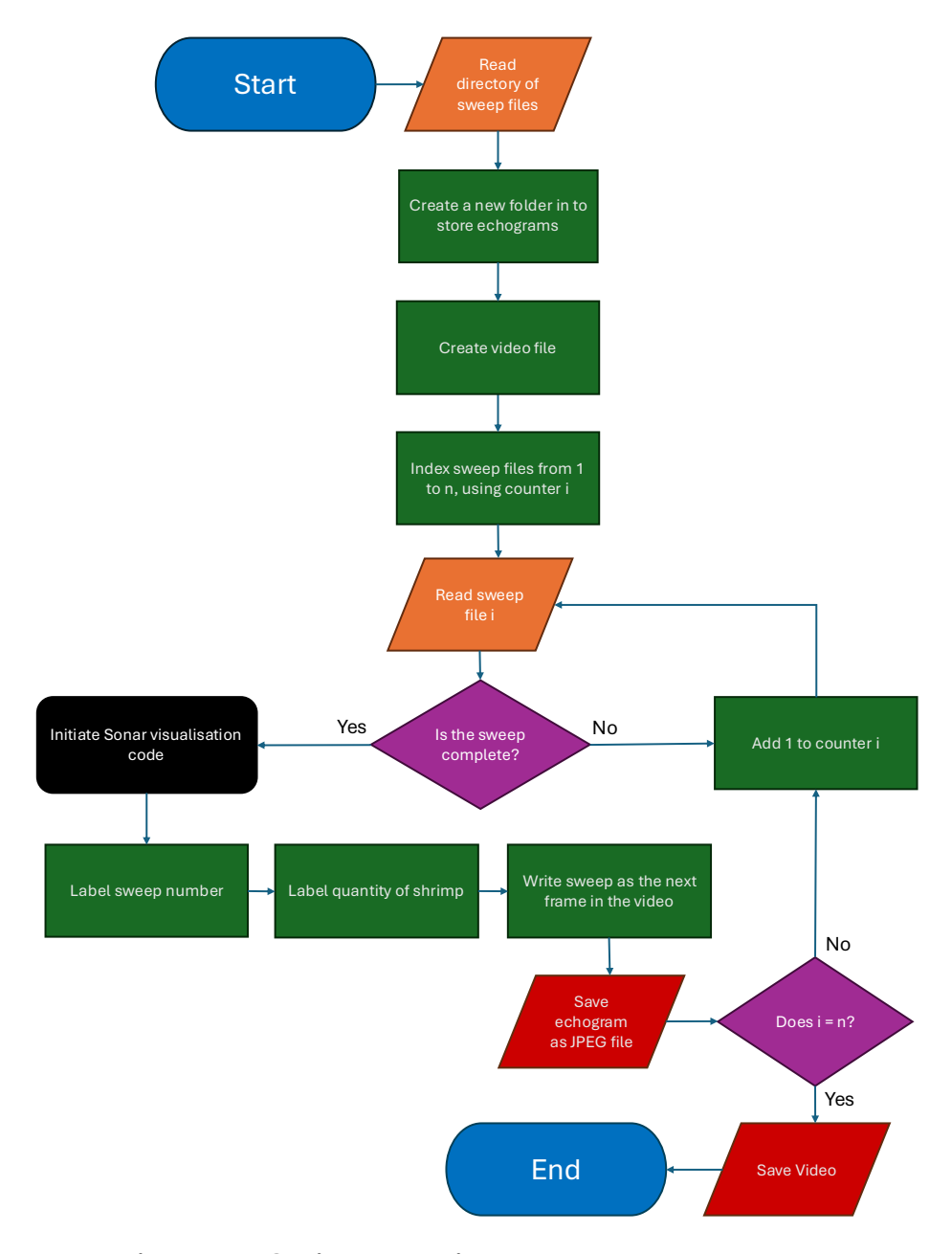


Figure 18 - Shrimp data time-lapse code flowchart

```
Code:
% Sonar Scanner v2: incomplete log file patch
% - Description: This code returns Sonar Images for each sweep and compiles
% them into a video from log files contained in the current folder by
% typing SonarScanner in the command window
% *NOTE 1*: Ensure the current folder opened in MATLAB is the folder
containing the log
% files
% *NOTE 2*: In event of path error, simply add folder to the MATLAB path
% -----
% - Author: B.Eng. Hamzah Isap
% - Contact: hamzahisap02@gmail.com
% - Date: September 2024
% ------
function SonarScanner(Av)
   mkdir SonarScanImages
   files = dir('*.log'); % Convert log files to 3D array
   csweep = ones(400,257);
   for i=1:length(files) %2:(length(files)-1)
       T = readtable(files(i).name, Range="C1:IY400");
       if size(T,1) <= 399</pre>
           continue
       end
       csweep(:,:,i) = table2array(T);
   end
       idx = all(csweep == 1, [1 2]);
       id0 = all(csweep == 0, [1 2]);
       csweep(:,:,idx) = [];
       csweep(:,:,id0) = [];
   %b1 = repmat(1, [1 \ 24]); b2 = repmat(2, [1 \ 19]); b3 = repmat(3, [1 \ 24]);
b4 = repmat(4, [1 24]); b0 = repmat(0, [1 13]);
   %bn = [b1 b2 b3 b4 b0];
   cd SonarScanImages % Create files inside folder 'SonarScanImages'
   v = VideoWriter("SonarScans", "MPEG-4");
   v.FrameRate = 2; % Set fps
   open(v)
   for i = 1:length(files) %2:(length(files)-1)
       sonar(csweep(:,:,i))%, 'average', Av) % Use the sonar command to
produce images
       %title(sprintf("balls: %d, sweep no: %d", bn(i),i))
       set(gcf, 'Units', 'Normalized', 'OuterPosition', [0, 0.04, 1, 0.96]);
       saveas(gcf,sprintf('sonarscan_%d.jpg',i)) % Image number corresponds
to sweep number
       frame = getframe(gcf);
       writeVideo(v,frame) % create video from string of images
       clf
```

end
close(v)

References

- [1] O. Mendoza *et al*, "Metagenomic Analyses of Biofilms on Whiteleg Shrimp (Litopenaeus vannamei) Effluents: Implications for Worldwide Aquaculture Bioremediation and Environmental Sustainability in the Current Trend of Climate Change and Global Warming State of the Art and Experimental Proof of Concept," *Reviews in Fisheries Science*, vol. 29, *(4)*, pp. 431–444, 2021. Available: https://www.tandfonline.com/doi/abs/10.1080/23308249.2020.1820720. DOI: 10.1080/23308249.2020.1820720.
- [2] E. K. Pikitch, D. D. Huppert and M. P. Sissenwine, "Fisheries Management," 1994. .
- [3] M. S. Hossain, M. J. Uddin and A. N. M. Fakhruddin, "Impacts of shrimp farming on the coastal environment of Bangladesh and approach for management," *Rev Environ Sci Biotechnol*, vol. 12, *(3)*, pp. 313, 2013. . DOI: 10.1007/s11157-013-9311-5.
- [4] F. Pa ´ez-Osuna, "The Environmental Impact of Shrimp Aquaculture: Causes, Effects, and Mitigating Alternatives," *Environmental Management*, vol. 28, (1), pp. 131, 2001.. DOI: 10.1007/s002670010212.
- [5] M. G. C. Emerenciano *et al*, "Intensification of Penaeid Shrimp Culture: An Applied Review of Advances in Production Systems, Nutrition and Breeding," *Animals*, vol. 12, *(3)*, 2022. . DOI: 10.3390/ani12030236.
- [6] D. Li, Y. Hao and Y. Duan, "Nonintrusive methods for biomass estimation in aquaculture with emphasis on fish: a review," *Reviews in Aquaculture*, vol. 12, *(3)*, pp. 1390, 2019. . DOI: 10.1111/raq.12388.
- [7] C. R. Engle *et al*, "Economics of Sustainable Intensification of Aquaculture: Evidence from Shrimp Farms in Vietnam and Thailand," *J World Aquaculture Soc*, vol. 48, *(2)*, pp. 227, 2017. . DOI: 10.1111/jwas.12423.
- [8] R. Yu, P. Leung and P. Bienfang, "Predicting shrimp growth: Artificial neural network versus nonlinear regression models," *Aquacultural Engineering*, vol. 34, (1), pp. 26–32, 2006. Available: https://dx.doi.org/10.1016/j.aquaeng.2005.03.003. DOI: 10.1016/j.aquaeng.2005.03.003.
- [9] G. Bardera *et al*, "The influence of density and dominance on Pacific white shrimp (Litopenaeus vannamei) feeding behaviour," *Aquaculture*, vol. 531, 2020. . DOI: 10.1016/j.aquaculture.2020.735949.
- [10] G. W. Klontz and H. Kaiser, "Producing a marketable fish, part V: inventory techniques: three tried-and-true methods for sampling pond populations of farmed salmonids," *Northern Aquaculture*, vol. 9, (2), pp. 21, 1993. Available: https://www.proquest.com/docview/201688518.

- [11] V. F. Matveev, "Assessing the biomass of small fish with a split-beam sonar in the Murray River, Australia," *Fisheries Research*, vol. 88, *(1-3)*, pp. 139, 2007. . DOI: 10.1016/j.fishres.2007.07.008.
- [12] S. G. Conti *et al*, "Acoustical monitoring of fish density, behavior, and growth rate in a tank," *Aquaculture*, vol. 251, *(2-4)*, pp. 314, 2006. . DOI: 10.1016/j.aquaculture.2005.06.018.
- [13] J. De Rosny and P. Roux, "Multiple scattering in a reflecting cavity: Application to fish counting in a tank," *The Journal of the Acoustical Society of America*, vol. 109, *(6)*, pp. 2587, 2001. . DOI: 10.1121/1.1369101.
- [14] M. Føre et al, "Precision fish farming: A new framework to improve production in aquaculture," *Biosystems Engineering*, vol. 173, pp. 176, 2017. . DOI: 10.1016/j.biosystemseng.2017.10.014.
- [15] D. Li et al, "Automatic counting methods in aquaculture: A review," *J World Aquaculture Soc*, vol. 52, (2), pp. 269, 2020. . DOI: 10.1111/jwas.12745.
- [16] Y. Chai et al, "Deep Learning Algorithms for Sonar Imagery Analysis and Its Application in Aquaculture: A Review," *IEEE Sensors J.*, vol. 23, *(23)*, pp. 28549, 2023. . DOI: 10.1109/jsen.2023.3324438.
- [17] D. Li *et al*, "Recent advances in acoustic technology for aquaculture: A review," *Reviews in Aquaculture*, vol. 16, *(1)*, pp. 357, 2023. . DOI: 10.1111/raq.12842.
- [18] J. Simmonds and D. N. MacLennan, *Fisheries Acoustics*. (2nd ed. ed.) 2008*10*Available:

http://portal.igpublish.com/iglibrary/search/WILEYB0014124.html.

- [19] J. Ehrenberg, "Echo counting and echo integration with a sector scanning sonar," *Journal of Sound and Vibration*, vol. 73, *(3)*, pp. 321–332, 1980. Available: https://dx.doi.org/10.1016/0022-460X(80)90517-9. DOI: 10.1016/0022-460X(80)90517-9.
- [20] J. Wang *et al*, "Deep learning for smart manufacturing: Methods and applications," *Journal of Manufacturing Systems*, vol. 48, pp. 144, 2018. . DOI: 10.1016/j.jmsy.2018.01.003.
- [21] F. Lin *et al*, "Development of ultrasonic shrimp monitoring system based on machine learning approaches," in Oct 10, 2022, Available: https://ieeexplore.ieee.org/document/9958877. DOI: 10.1109/IUS54386.2022.9958877.
- [22] M. K. Pargi *et al*, "Improving aquaculture systems using AI: Employing predictive models for biomass estimation on sonar images," in 2022-12, . DOI: 10.1109/icmla55696.2022.00250.

- [23] A. Minelli *et al*, "Semi-Automated Data Processing and Semi-Supervised Machine Learning for the Detection and Classification of Water-Column Fish Schools and Gas Seeps with a Multibeam Echosounder," *Sensors (Basel, Switzerland)*, vol. 21, (9), pp. 2999, 2021. Available: https://www.ncbi.nlm.nih.gov/pubmed/33923343. DOI: 10.3390/s21092999.
- [24] R. Proud *et al*, "Automated classification of schools of the silver cyprinid Rastrineobola argentea in Lake Victoria acoustic survey data using random forests," *ICES Journal of Marine Science*, vol. 77, *(4)*, pp. 1379–1390, 2020. Available: https://academic.oup.com/icesjms/article-pdf/77/4/1379/33513175/fsaa052.pdf. DOI: 10.1093/icesjms/fsaa052.
- [25] F. Asche et al, "The economics of shrimp disease," *Journal of Invertebrate Pathology*, vol. 186, pp. 107397, 2021. Available: https://dx.doi.org/10.1016/j.jip.2020.107397. DOI: 10.1016/j.jip.2020.107397.
- [26] M. J. Hasan *et al*, "Exploring the Feasibility of Affordable Sonar Technology: Object Detection in Underwater Environments Using the Ping 360," 2024. Available: https://arxiv.org/abs/2411.05863. DOI: 10.48550/arxiv.2411.05863.
- [27] V. Hatje *et al*, "Detection of environmental impacts of shrimp farming through multiple lines of evidence," *Environmental Pollution*, vol. 219, pp. 672, 2016. . DOI: 10.1016/j.envpol.2016.06.056.
- [28] P. Singh *et al*, *Shrimp Culture Technology*. (1st ed. 2025 ed.) 2025Available: https://doi.org/10.1007/978-981-97-8549-0.
- [29] M. S. R. Licop, "Sodium-EDTA effects on survival and metamorphosis of Penaeus monodon larvae," *Aquaculture*, vol. 74, *(3-4)*, pp. 239–247, 1988. .
- [30] M. B. New, "Farming freshwater prawns. A manual for the culture of the giant river prawn (macrobrachium rosenbergii)," in *FAO Fisheries Technical Paper*Anonymous 2005, Available:

https://search.proquest.com/docview/19681127.

- [31] D. V. Smith and S. Tabrett, "The use of passive acoustics to measure feed consumption by Penaeus monodon (giant tiger prawn) in cultured systems," *Aquacultural Engineering*, vol. 57, pp. 38, 2013. . DOI: 10.1016/j.aquaeng.2013.06.003.
- [32] M. Irani *et al*, "Production of Pacific white shrimp under different stocking density in a zero-water exchange biofloc system: Effects on water quality, zootechnical performance, and body composition," *Aquacultural Engineering*, vol. 100, 2022. . DOI: 10.1016/j.aquaeng.2022.102313.
- [33] X. Yang *et al*, "Deep learning for smart fish farming: applications, opportunities and challenges," *Reviews in Aquaculture*, vol. 13, *(1)*, pp. 66, 2020. . DOI: 10.1111/raq.12464.

- [34] T. Wuest *et al*, "Machine learning in manufacturing: advantages, challenges, and applications," *Production & Amp; Manufacturing Research*, vol. 4, *(1)*, pp. 23, 2016. DOI: 10.1080/21693277.2016.1192517.
- [35] F. Lin *et al*, "Development of ultrasonic shrimp monitoring system based on machine learning approaches," in 2022-10-10, . DOI: 10.1109/ius54386.2022.9958877.
- [36] Y. Huang, W. Li and F. Yuan, "Speckle Noise Reduction in Sonar Image Based on Adaptive Redundant Dictionary," *JMSE*, vol. 8, *(10)*, 2020. . DOI: 10.3390/jmse8100761.
- [37] H. Liang, G. Hao and O. Z. Olszewski, "A review on vibration-based piezoelectric energy harvesting from the aspect of compliant mechanisms," *Sensors and Actuators A: Physical*, vol. 331, 2021. . DOI: 10.1016/j.sna.2021.112743.
- [38] R. J. Urick, *Principles of Underwater Sound*. (3rd ed ed.) Peninsula publishing, 1983.
- [39] J. M. Hovem, "Underwater acoustics: Propagation, devices and systems," in 2007-02-21, . DOI: 10.1007/s10832-007-9059-9.
- [40] K. M. Boswell *et al*, "Evaluation of target strength–fish length equation choices for estimating estuarine fish biomass," *Hydrobiologia*, vol. 610, *(1)*, pp. 113, 2008. . DOI: 10.1007/s10750-008-9425-x.
- [41] A. C. Lavery *et al*, "Three-dimensional modeling of acoustic backscattering from fluid-like zooplankton," *The Journal of the Acoustical Society of America*, vol. 111, (3), pp. 1197, 2002. DOI: 10.1121/1.1433813.
- [42] S. Fraser, "Acoustic Investigation of the Hydrodynamics and Ecology of a Tidal Channel and the Impacts of a Marine Renewable Energy Installation.", ProQuest Dissertations & Theses, 2017.
- [43] E. J. Simmonds, "The effects of mounting the equivalent beam angle of acoustic survey transducers," in Jan 1, 1984, Available: https://search.proquest.com/docview/14277181.
- [44] SIMMONDS E. J, "A comparison between measured and theoretical equivalent beam angles for seven similar transducers," *J. Sound Vib*, vol. 97, pp. 117–128, 1984. .
- [45] F. R. Knudsen and H. Sægrov, "Benefits from horizontal beaming during acoustic survey: application to three Norwegian lakes," *Fisheries Research*, vol. 56, *(2)*, pp. 205, 2018. . DOI: 10.1016/s0165-7836(01)00318-6.

- [46] M. V. Trevorrow, "Salmon and herring school detection in shallow waters using sidescan sonars," *Fisheries Research*, vol. 35, (1), pp. 5–14, 1998. Available: https://dx.doi.org/10.1016/S0165-7836(98)00054-X. DOI: 10.1016/s0165-7836(98)00054-x.
- [47] J. Kubecka and M. Wittingerova, "Horizontal beaming as a crucial component of acoustic fish stock assessment in freshwater reservoirs," *Fisheries Research*, vol. 35, (1), pp. 99–106, 1998. Available: https://dx.doi.org/10.1016/S0165-7836(98)00064-2. DOI: 10.1016/S0165-7836(98)00064-2.
- [48] S. G. Conti and D. A. Demer, "Wide-bandwidth acoustical characterization of anchovy and sardine from reverberation measurements in an echoic tank," *ICES Journal of Marine Science*, vol. 60, *(3)*, pp. 617, 2003. DOI: 10.1016/s1054-3139(03)00056-0.
- [49] O. Dragesund and S. Olsen, "On the possibility of estimating year-class strength by measuring echo-abundance of 0-group fish," in *Fiskeridirektoratets Skrifter*. *Serie Havundersoekelser*Anonymous 1965, Available: https://search.proquest.com/docview/18888914.
- [50] O. A. Misund *et al*, "Improved mapping of schooling fish near the surface: comparison of abundance estimates obtained by sonar and echo integration," *ICES Journal of Marine Science*, vol. 53, *(2)*, pp. 383–388, 1996. Available: https://api.istex.fr/ark:/67375/HXZ-J31XC92K-D/fulltext.pdf. DOI: 10.1006/jmsc.1996.0053.
- [51] H. Liu *et al*, "Application of Deep Learning-Based Object Detection Techniques in Fish Aquaculture: A Review," *Journal of Marine Science and Engineering*, vol. 11, *(4)*, pp. 867, 2023. Available: https://www.proquest.com/docview/2806556124. DOI: 10.3390/jmse11040867.
- [52] H. Kim *et al*, "Acoustic Target Strength Measurements for Biomass Estimation of Aquaculture Fish, Redlip Mullet (Chelon haematocheilus)," *Applied Sciences*, vol. 8, *(9)*, pp. 1536, 2018. Available: https://www.proquest.com/docview/2321991425. DOI: 10.3390/app8091536.
- [53] F. O'Donncha *et al*, "Data Driven Insight Into Fish Behaviour and Their Use for Precision Aquaculture," *Frontiers in Animal Science*, vol. 2, 2021. Available: https://www.frontiersin.org/articles/10.3389/fanim.2021.695054/pdf. DOI: 10.3389/fanim.2021.695054.
- [54] J. Kristmundsson *et al*, "Fish Monitoring in Aquaculture Using Multibeam Echosounders and Machine Learning," *IEEE Access*, vol. 11, pp. 108306, 2023. . DOI: 10.1109/access.2023.3320949.
- [55] Z. Guan *et al*, "Design and research of uniform linear array for imaging sonar," in Sep 2019, Available: https://ieeexplore.ieee.org/document/8960731. DOI: 10.1109/ICSPCC46631.2019.8960731.

- [56] D. V. Smith and M. S. Shahriar, "A context aware sound classifier applied to prawn feed monitoring and energy disaggregation," *Knowledge-Based Systems*, vol. 52, pp. 21, 2013. . DOI: 10.1016/j.knosys.2013.05.007.
- [57] J. Darodes De Tailly *et al*, "Monitoring methods of feeding behaviour to answer key questions in penaeid shrimp feeding," *Reviews in Aquaculture*, vol. 13, *(4)*, pp. 1828, 2021.. DOI: 10.1111/raq.12546.
- [58] T. T. T. Nguyen and G. Armitage, "A survey of techniques for internet traffic classification using machine learning," *COMST*, vol. 10, *(4)*, pp. 56–76, 2008. Available: https://ieeexplore.ieee.org/document/4738466. DOI: 10.1109/SURV.2008.080406.
- [59] A. Yassir *et al*, "Acoustic fish species identification using deep learning and machine learning algorithms: A systematic review," *Fisheries Research*, vol. 266, pp. 106790, 2023. Available: https://dx.doi.org/10.1016/j.fishres.2023.106790. DOI: 10.1016/j.fishres.2023.106790.
- [60] S. A. Villar *et al*, "ECOPAMPA: A new tool for automatic fish schools detection and assessment from echo data," *Heliyon*, vol. 7, (1), pp. e05906, 2021. Available: https://dx.doi.org/10.1016/j.heliyon.2021.e05906. DOI: 10.1016/j.heliyon.2021.e05906.
- [61] S. Aronica *et al*, "Identifying small pelagic Mediterranean fish schools from acoustic and environmental data using optimized artificial neural networks," *Ecological Informatics*, vol. 50, pp. 149–161, 2019. Available: https://dx.doi.org/10.1016/j.ecoinf.2018.12.007. DOI: 10.1016/j.ecoinf.2018.12.007.
- [62] M. Sung et al, "Realistic Sonar Image Simulation Using Deep Learning for Underwater Object Detection," *Int. J. Control Autom. Syst*, vol. 18, *(3)*, pp. 523–534, 2020. Available: https://link.springer.com/article/10.1007/s12555-019-0691-3. DOI: 10.1007/s12555-019-0691-3.
- [63] E. L. Hazen and J. K. Horne, "A method for evaluating the effects of biological factors on fish target strength," *ICES Journal of Marine Science*, vol. 60, (3), pp. 555–562, 2003. Available: https://api.istex.fr/ark:/67375/HXZ-MQWZTP72-Q/fulltext.pdf. DOI: 10.1016/S1054-3139(03)00053-5.
- [64] O. Nakken and K. Olsen, "Target strength measurements of fish," 1977. Available: http://hdl.handle.net/11250/107967.
- [65] K. G. Foote, "Importance of the swimbladder in acoustic scattering by fish: A comparison of gadoid and mackerel target strengths," *The Journal of the Acoustical Society of America*, vol. 67, (6), pp. 2084–2089, 1980. Available: https://search.proquest.com/docview/15236425. DOI: 10.1121/1.384452.

- [66] T. K. Stanton, D. Chu and P. H. Wiebe, "Acoustic scattering characteristics of several zooplankton groups," *ICES Journal of Marine Science*, vol. 53, *(2)*, pp. 289–295, 1996. Available: https://api.istex.fr/ark:/67375/HXZ-1H0D95HM-Z/fulltext.pdf. DOI: 10.1006/jmsc.1996.0037.
- [67] R. J. Korneliussen *et al*, "ICES COOPERATIVE RESEARCH REPORT #344," 2018.
- [68] A. C. Lavery *et al*, "Three-dimensional modeling of acoustic backscattering from fluid-like zooplankton," *The Journal of the Acoustical Society of America*, vol. 111, *(3)*, pp. 1197–1210, 2002. Available: https://www.ncbi.nlm.nih.gov/pubmed/11931297. DOI: 10.1121/1.1433813.
- [69] The Scuba Diver Store. *JW Fishers SCAN 650 Scanning Sonar*. Available: https://www.thescubadiverstore.com/product/jw-fishers-scan-650-scanning-sonar/.
- [70] Carcinus Ltd. *Blue Robotics Ping360 Scanning Imaging Sonar*. Available: https://www.carcinus.co.uk/product/ping360-scanning-imaging-sonar/?utm_source=adwords&utm_term=&utm_campaign=Blue+Robotics+-+Shopping+Std&utm_medium=ppc&hsa_kw=&hsa_ad=695390233902&hsa_src=g&hsa_ver=3&hsa_grp=162959131080&hsa_cam=20071001649&hsa_tgt=pla-362587409677&hsa_acc=3301071309&hsa_mt=&hsa_net=adwords&gad_source=1&gclid=Cj0KCQjwhr6_BhD4ARIsAH1YdjDBtM11GPkhRf75rc9OK_OyFZ1jE0SBESyGVDo-IYbwhOMVRqe8nDMaAnupEALw_wcB.
- [71] L. Zhang *et al*, "Automatic shrimp counting method using local images and lightweight YOLOv4," *Biosystems Engineering*, vol. 220, pp. 39–54, 2022. Available: https://dx.doi.org/10.1016/j.biosystemseng.2022.05.011. DOI: 10.1016/j.biosystemseng.2022.05.011.
- [72] T. K. Stanton *et al*, "Sound scattering by several zooplankton groups. I. Experimental determination of dominant scattering mechanisms," *The Journal of the Acoustical Society of America*, vol. 103, *(1)*, pp. 225–235, 1998. Available: https://www.ncbi.nlm.nih.gov/pubmed/9440325. DOI: 10.1121/1.421469.
- [73] E. Caló and V. V. Khutoryanskiy, "Biomedical applications of hydrogels: A review of patents and commercial products," *European Polymer Journal*, vol. 65, pp. 252–267, 2015. Available: https://dx.doi.org/10.1016/j.eurpolymj.2014.11.024. DOI: 10.1016/j.eurpolymj.2014.11.024.
- [74] S. Casciaro *et al*, "Experimental investigation and theoretical modelling of the nonlinear acoustical behaviour of a liver tissue and comparison with a tissue mimicking hydrogel," *J Mater Sci: Mater Med*, vol. 19, *(2)*, pp. 899–906, 2008. Available: https://link.springer.com/article/10.1007/s10856-007-3007-8. DOI: 10.1007/s10856-007-3007-8.

[75] H. M and S. M.N, "A Review on Evaluation Metrics for Data Classification Evaluations," *International Journal of Data Mining & Knowledge Management Process*, vol. 5, *(2)*, pp. 1–11, 2015. Available: https://doi.org/10.5121/ijdkp.2015.5201. DOI: 10.5121/ijdkp.2015.5201.

[76] Supertex inc, "High Speed, Dual MOSFET Datasheet," Microchip Technology,

2012. Available: https://www.microchip.com/en-us/product/md1211.

[77] N. Castillo, "Application of Lookup Tables and their implementation FPGAs," .